HHS Public Access

Author manuscript

Toxicol Appl Pharmacol. Author manuscript; available in PMC 2018 May 01.

Published in final edited form as:

Toxicol Appl Pharmacol. 2017 May 01; 322: 60–74. doi:10.1016/j.taap.2017.02.020.

In vitro cardiotoxicity assessment of environmental chemicals using an organotypic human induced pluripotent stem cell-derived model

Oksana Sirenko[*], **Fabian A. Grimm**[†], **Kristen R. Ryan**[‡], **Yasuhiro Iwata**[†], **Weihsueh A. Chiu**[†], **Frederick Parham**[‡], **Jessica A. Wignall**[§], **Blake Anson**[¶], **Evan F. Cromwell**[‖], **Mamta Behl**[‡], **Ivan Rusyn**[†], and **Raymond R. Tice**[‡]

[*]Molecular Devices, LLC, Sunnyvale, CA

[†]Department of Veterinary Integrative Biosciences, Texas A&M University, College Station, TX

[‡]Division of the National Toxicology Program, National Institute of Environmental Health Sciences, Research Triangle Park, NC

[§]ICF International, Fairfax, VA

[¶]Cellular Dynamics International, Madison, WI

[‖]Protein Fluidics, Inc., Hayward, CA

Abstract

An important target area for addressing data gaps through *in vitro* screening is the detection of potential cardiotoxicants. Despite the fact that current conservative estimates relate at least 23% of all cardiovascular disease cases to environmental exposures, the identities of the causative agents remain largely uncharacterized. Here, we evaluate the feasibility of a combinatorial *in vitro/in silico* screening approach for functional and mechanistic cardiotoxicity profiling of environmental hazards using a library of 69 representative environmental chemicals and drugs. Human induced pluripotent stem cell-derived cardiomyocytes were exposed in concentration-response for 30 min or 24 hrs and effects on cardiomyocyte beating and cellular and mitochondrial toxicity were assessed by kinetic measurements of intracellular Ca^{2+} flux and high-content imaging using the nuclear dye Hoechst 33342, the cell viability marker Calcein AM, and the mitochondrial depolarization probe JC-10. More than half of tested chemicals exhibited effects on cardiomyocyte rhythm after 30 min of exposure. After 24 hours, the effects on cell rhythm without cytotoxicity were observed in about one third of the compounds. Concentration-response data for *in vitro* bioactivity phenotypes were visualized using Toxicological Prioritization Index (ToxPi) and showed chemical class-specific clustering of environmental chemicals, including pesticides, flame retardants, and polycyclic aromatic hydrocarbons. For environmental chemicals with human

Address correspondence to: Oksana Sirenko, PhD, Molecular Devices, LLC, 1311 Orleans Drive, Sunnyvale, CA 94089, USA, oksana.sirenko@moldev.com.

Conflict of Interest Statement

Oksana Sirenko is currently employed and Evan F Cromwell was employed by Molecular Devices, which provides instrumentation and reagents for the high-content screening assays. Blake Anson is employed by Cellular Dynamics International, a provider of iPSC-derived cells.

exposure predictions, the activity-to-exposure ratios between modeled blood concentrations and *in vitro* bioactivity were between one and five orders of magnitude. These findings not only demonstrate that some ubiquitous environmental pollutants might have the potential to alter cardiomyocyte function at high exposures, but also indicate similarities in the mechanism of these effects both within and among chemicals and classes.

Keywords

Environmental Toxicology; Cardiotoxicity; Cardiomyocytes; High-Content Screening; Induced pluripotent stem cells; Alternative Methods

1. Introduction

A large number of environmental agents remain inadequately tested for their potential toxicological effects (Judson *et al.* 2009). In the United States, the National Toxicology Program at the National Institute of Environmental Health Sciences, the Environmental Protection Agency, the National Center for Advancing Translational Science, and the Food and Drug Administration are addressing toxicity data needs through the Tox21 collaboration, an initiative to implement novel *in vitro* screening for thousands of chemicals (Collins *et al.* 2008; Tice *et al.* 2013).

Important target areas for addressing data gaps through *in vitro* screening include the detection of potential cardiotoxic effects. Despite the fact that current conservative estimates relate at least 23% of all cardiovascular disease cases to environmental exposures, the identities of the causative environmental agents remain largely uncharacterized (Pruss-Ustun and Corvalan 2006). Moreover, cardiotoxicity remains among one of the most pronounced reasons, comparable to those associated with hepatotoxicity, for drug attrition during clinical trials and post-marketing (Berridge *et al.* 2013; Laverty *et al.* 2011; Nadanaciva and Will 2011; Pierson *et al.* 2013). Current pre-clinical approaches for cardiophysiologic evaluations of chemicals rely almost exclusively on large animal models and this approach has significant limitations in terms of the cost and complexity of the studies (Herman and Ferrans 1998). Hence, there is a pressing need for the development of comprehensive, multi-parametric screening strategies that provide improved predictability of cardiotoxic effects (Roberts *et al.* 2014). In order to capture the wide range of potential cardiotoxic effects, novel approaches need to rely on cardiomyocyte functional assays, not just traditional cytotoxicity measurements, because interference with normal cellular electrophysiology as well as sub-cytotoxic perturbation of biochemical pathways can impact on contractility and organ function (Chen *et al.* 2016).

As an alternative to primary cardiomyocytes and myocardial tissue preparations, human inducible pluripotent stem cell (iPSC)-derived *in vitro* model systems have more recently emerged as a physiologically-relevant and highly reproducible option for cardiotoxicity testing (Guo *et al.* 2013; Ma *et al.* 2011; Mercola *et al.* 2013; Suter-Dick *et al.* 2015). iPSC-derived cardiomyocytes are a particularly attractive *in vitro* model as they form a synchronously beating monolayer that can be used to reliably reproduce drug-associated cardiophysiologic phenotypes using a fast kinetic fluorescence assay that monitors changes

in intracellular Ca^{2+} flux (Grimm *et al*. 2016; Sirenko *et al*. 2013a; Sirenko *et al*. 2013b). This approach is amenable to quantitative multi-parametric assessment of various phenotypes, e.g. positive and negative inotropic effects and prolonged repolarization, in medium- to high-throughput screening formats (Grimm *et al*. 2015). Of particular interest is the ability to use iPSC-derived cardiomyocytes to test for the potential of chemicals to induce cardiac arrhythmias because interference with cardiomyocyte repolarization, i.e. the *in vitro* equivalent to clinical QT prolongation, has been a useful phenotype easily observable *in vitro* (Blinova *et al*. 2017). A study evaluating 131 drugs demonstrated that a comprehensive concentration-response assessment of multiple functional read-outs yields predictive and mechanistically-interpretable data on cardiotoxicity, thereby indicating its potential applicability to evaluate and prioritize environmental chemicals for this important endpoint (Sirenko *et al*. 2013b).

In this study, we evaluated the utility of multiplexed functional *in vitro* assays in iPSC-derived cardiomyocytes for the high-throughput screening of several diverse classes of environmental chemicals as well as drugs; some of the environmental chemicals have been associated with suspected cardiotoxicity potential (Kaufman *et al*. 1992; Zafiropoulos *et al*. 2014; Zhang *et al*. 2013). We used Ca^{2+} flux measurements in combination with high-content imaging to evaluate concentration-dependent effects on cardiomyocyte physiology, mitochondrial membrane potential, and cell viability. Benchmark concentration point-of-departure (POD) values were utilized for bioactivity grouping and ranking of the chemicals in Toxicological Prioritization Index Graphical User Interface (ToxPi GUI) software (Reif *et al*. 2013).

2. Materials and methods

The overall experimental design is shown in Figure 1.

2.1. Chemical library

The library used in these studies is comprised of 69 unique chemicals (Table 1) with mostly limited or unknown evidence for cardiotoxicity. These chemicals were provided by the National Toxicology Program at the National Institute of Environmental Health Sciences and information on their purity and supplier is provided in Supplementary Table 1. This set was selected to broadly reflect diverse chemical classes and included drugs (n=18), pesticides (n=15), flame retardants (n=10), polycyclic aromatic hydrocarbons (PAHs; n=14), and 12 chemicals classified as “other”. All tests described in the article were performed as duplicates. Four of these chemicals (deltamethrin, triphenyl phosphate, methyl mercuric (II) chloride, saccharin) were also tested in additional replicates on each microplate to assess assay-specific inter-plate replicability. In addition, assay-specific cardiotoxicity positive (antimycin A, digoxin, carbonyl cyanide m-chlorophenyl hydrazine (CCCP)) and negative (biotin, sorbitol, adipic acid) control chemicals (all from Sigma, St. Louis, MO, USA) were included in the screening (Table 1). Stock solutions (20 mM) of all chemicals were prepared in cell-culture grade dimethyl sulfoxide (DMSO, Sigma) and stored at −20°C. Vehicle (n=30-38, DMSO concentration of 0.15% v/v) and untreated (media only) wells were

included on each assay plate and used for normalization of plate-specific readouts and quality control.

2.2. *In silico* assessment of chemical diversity

Diversity among chemicals included in the screening library, as compared to a curated dataset of 32,464 unique environmental chemicals and drugs described in Mansouri *et al.* (2016), was assessed by principal components analysis (PCA) using *in silico*-derived physico-chemical descriptors. PCA was conducted using the *gplots* package in R studio. Supplementary Table 2 contains a list of the 153 chemical descriptors obtained using the Chemistry Development Kit (CDK) (Steinbeck *et al.* 2003).

2.3. Cell culture

Human iPSC-derived cardiomyocytes (iCell™ cardiomyocytes), plating medium, and maintenance medium were provided by Cellular Dynamics International (Madison, WI, USA). Cells were plated and maintained according to the manufacturer's recommendations as described previously (Sirenko *et al.* 2013a). Cells were plated into gelatin coated wells at 8,000 cells/well in 384 multi-well plates. Synchronous beating of cells was evident after 7 days of culture and experiments were conducted 12-14 days post-plating on plates when all wells demonstrated regular synchronous beating.

2.4. Calcium flux assay

The intracellular Ca^{2+}-flux in cardiomyocytes was assessed at 30 min and 24 hrs using the EarlyTox® Cardiotoxicity kit (Molecular Devices, Sunnyvale, CA, USA) as described in detail elsewhere (Grimm *et al.* 2015; Sirenko *et al.* 2013a). For both time points, chemicals were tested using a single exposure in duplicate at concentrations ranging from 0.3 to 100 μM with semi-log dilutions. Fluorescent measurements of intracellular Ca^{2+}-flux were accomplished using the FLIPR® tetra high-throughput cellular screening system combined with a TetraCycler® Microplate Handler (Molecular Devices). Final DMSO concentrations were 0.15% (v/v) with the exception of 100 μM concentration data point where DMSO concentration was 0.5%. Prior to treatment with test chemicals, basal kinetics of intracellular Ca^{2+}-flux was determined in each well. Peak frequency (beats per minute), peak width (at 10% amplitude), peak spacing, peak amplitude, peak rise time (from 10% to 90% amplitude), and peak decay time (from 90% to 10% amplitude) were derived using the ScreenWorks® Peak Pro® software (Molecular Devices). Based on previous data showing that peak amplitude data are highly variable (Sirenko *et al.*, 2013b), this parameter was not evaluated.

2.5. Cell viability imaging

To evaluate cytotoxicity, Calcein AM (final concentration 0.5 μM) measurements were performed at 30 min and 24 hrs. All conditions were as detailed elsewhere (Grimm *et al.* 2015; Sirenko *et al.* 2013a). In a separate experiment to assess effects on mitochondrial integrity, cells were treated with chemicals for 30 min and co-stained with Hoechst 33342 (2 μg/ml) and the mitochondria-specific dye JC-10 (AAT Bioquest, Sunnyvale, CA, USA) according to the manufacturer's instructions. All images were acquired using the

ImageXpress® Micro XL instrument (Molecular Devices) and were processed and quantified using the Multi-Wavelength Cell Scoring and Granularity application modules in MetaXpress® software (Molecular Devices). Read-outs included nuclei count and intensity for Hoechst 33342, percent live cells and total area of live cells for Calcein AM, and the number of mitochondrial granules per cell and average mitochondrial granule area and intensity for JC-10.

2.6. Concentration-response assessment

For quantitative toxicity profiling, we normalized phenotype and plate-specific readouts to their respective vehicle controls. Normalized concentration-response data were fit to a four-parameter maximum-likelihood logistic model in R studio software (version 3.1.1) as described previously (Grimm *et al.* 2015; Sirenko *et al.* 2013b). We used a one standard deviation departure from the control mean as the benchmark concentration for deriving the POD. This value represents a minimum active concentration and is consistent with the US EPA guidance for dose-response modeling and determination of POD values using continuous data types (U.S. EPA 2012). If the maximum response did not reach this level in the concentration range tested, the “no observable adverse effect level” was recorded as the highest concentration tested (100 μM at 30 min or 30 μM at 24 hrs, i.e., the 100 μM data at 24 hrs were excluded due to excessive variability). Identical curve fitting and POD derivation procedures were applied to all chemicals and phenotypes collected. All curve fits were visually examined and in cases of a non-monotonic dose-response, concentrations at which a change in monotonic slope was observed (outliers) were excluded and curve fitting was repeated. An overview of representative concentration-response curves, data integration, and processing can be found in Supplementary Figure 1.

2.7. Data integration

For global ranking and qualitative comparison of cardiotoxic potentials of the chemicals screened in this study, POD values were integrated and visualized using the Toxicological Priority Index Graphical User Interface (ToxPi GUI) (Reif *et al.* 2013). POD values for all 18 cardiophysiological and cellular/mitochondrial toxicity phenotypes were each normalized and scaled from 0 to 1 using logPOD which more appropriately represents changes across several orders of magnitude. The values of 0 reflect the highest observed POD or the highest tested concentration for nontoxic chemicals (100 μM at 30 min, 30 μM at 24 hrs) and the value of 1 reflects the lowest observed POD value, i.e. the most potent chemical with lowest POD, for each individual phenotype. The scaled POD values were then transferred into a ToxPi compatible data matrix and used to visualize chemical-specific bioactivity profiles. In the resulting pie charts, each slice is associated with a specific phenotype and the area covered by the slice is proportional to the relative toxicity of the chemical within this data set. In this approach, it is not possible to account for directionality; e.g., for the cell viability slice, chemicals that have a POD based on a decrease or an increase in Calcein AM signal are both included. ToxPi also derives a final ToxPi score, based on the sum of all eighteen slice areas, which we utilized as a measure for the relative toxicity of a given chemical and as a basis for global ranking of chemicals according to their cardiotoxic potential.

2.8. Assay quality control

The integrity and replicability of all screening assays were assessed using a variety of positive and negative quality controls. As a general measure for assay performance, we determined the coefficients of variation (%CV), herein defined as the ratio of one standard deviation and the means of the vehicle controls (n=164 for cardiophysiology phenotypes after 30 min; n=116 for cardiophysiology phenotypes after 24 hrs, including cell viability measurements; and n=144 for cellular and mitochondrial phenotypes). Inter-plate replicability was assessed using four chemicals: deltamethrin, triphenyl phosphate, methyl mercuric (II) chloride, and saccharin. Concentration-response determinations for all four chemicals and all phenotypes were repeated on both assay plates and used for quantitative comparison of their relative toxicities using derived POD values. Intra-plate replicability of duplicate determinations of all data points in this study was evaluated using Pearson and Spearman correlation analysis (Supplementary Table 3).

2.9. *In vitro*-to-*in vivo* extrapolation

For chemicals for which exposure and pharmacokinetic data are available, POD values were compared with estimated human *in vivo* blood concentrations. For pharmaceuticals, C_{max} values were extracted for this comparison from the PharmaPendium database. For the remaining compounds, steady state blood concentrations were estimated by combining exposure estimates from the U.S. EPA CompTox Chemistry Dashboard (https://comptox.epa.gov/dashboard) and toxicokinetic model predictions (Pearce *et al*. 2017; Wetmore *et al*. 2012; Wetmore *et al*. 2013). In all, human *in vivo* blood concentration estimates were available for about one half of the tested compounds (Supplementary Table 4). Conservative estimates for the margin of exposure were then derived by dividing the lowest POD value by the highest estimated human *in vivo* blood concentration.

3. Results

To evaluate the structural diversity of the 69 chemicals contained in the screening library, we conducted principal component analysis (PCA) based on 153 selected *in silico*-derived physico-chemical descriptors (Figure 2). Two-dimensional PCA (PC1 vs. PC2) revealed broad chemical diversity among the selected chemicals without clearly segregated clusters based on chemical classes. An exception to this observation was the relatively clear separation between the flame retardants and pesticides in this library. A comparison of the chemicals contained in the screening library with a broader chemical list encompassing 32,464 unique environmental chemicals and drugs that are part of the Collaborative Estrogen Receptor Activity Prediction Project (CERAPP) (Mansouri *et al*., 2016) showed the broad chemical diversity covered by the chemicals selected for screening in this study (Supplementary Figure 2).

Effects of test chemicals on cardiomyocyte beating were evaluated at 30 min and 24 hrs using five quantitative descriptors of intracellular Ca^{2+}-flux: peak frequency, width (at 10% peak amplitude), spacing between peaks, and peak rise and decay times. Examples of kinetic Ca^{2+} flux traces reflecting a wide range of effects of chemicals from diverse chemical classes on cardiomyocyte beating, including positive and negative inotropic effects and

prolonged repolarization, which is indicative of QT-interval prolongation in electrocardiographic measurements, are shown in Figure 3. Qualitative reference controls for various cardiophysiologic phenotypes included previously characterized cisapride and sotalol (potassium channel blockers, QT-interval elongation), as well as isoproterenol and verapamil (positive and negative inotropes). Negative- and positive control-induced phenotypes in all assays were in agreement with previous publications (Grimm *et al.* 2015; Sirenko *et al.* 2013a; Sirenko *et al.* 2013b).

Figure 3 also shows representative Ca^{2+}-flux traces for several compounds from each chemical class tested. Untreated and vehicle-only treated iPSC-derived cardiomyocytes exhibit a regular beating pattern that can be reproduced upon treatment with non-cardioactive control chemicals, e.g., biotin. Various drugs, including 1-methyl-4-phenylpyridinium and berberine chloride, have been shown to induce clinical QT-interval prolongation, which was reflected by a decrease in the peak frequency concomitant with an increase in the average peak width at 10% height of the peak amplitude. This pattern is characteristic for potassium channel inhibitors such as cisapride and sotalol, and is indicative of a chemical's ability to induce cardiac arrhythmias (Hancox *et al.* 2008; Jeyaraj *et al.* 2012; Knollmann 2013). A variety of environmental chemicals were capable of inducing positive inotropic effects, i.e., increases in peak frequency, ranging from mild (the PAHs benzo(e)pyrene and benzo(k)fluoranthene) and moderate (parathion, 2-ethylhexyl diphenyl phosphate) to very significant (2,2′,4,4′,5-tetrabromodiphenyl ether). Negative inotropic effects, i.e., decreases in peak frequency, were also observable for certain chemicals (rotenone). Positive and negative chronotropic effects are primarily associated with β-adrenergic receptor agonists and antagonists, and as such related to the physiological phenomena tachycardia and bradycardia (Hoekstra *et al.* 2012; Knollmann 2013; Li *et al.* 2013).

To quantify assay variability for different output parameters we used inter- and intra-plate replicate chemicals (Figure 4). As a general measure of assay quality, we determined the %CV for each of the eighteen phenotypes measured. Overall, %CV values for the cardiophysiology phenotypes and the cellular toxicity endpoints were below 10%, while the three mitochondrial phenotypes exhibiting higher levels of variability (from 13.4 to 23%, Figure 4A). Pearson (r) and Spearman (ρ) correlation analysis on duplicate determinations for both cardiophysiology and cellular and mitochondrial toxicity was performed to assess intra-plate replicability (Supplementary Table 3). For Ca^{2+} flux parameters, r values generally ranged between 0.75 and 0.83, with only peak spacing exhibiting a lower, yet highly significant, correlation (0.54). Spearman correlation values ranged between 0.72 and 0.83. For cellular and mitochondrial toxicity phenotypes, r values ranged between 0.82 and 0.99 and ρ values between 0.49 and 0.78. For all phenotypes, the correlations were significant ($p<0.0001$).

Inter-plate replicability was evaluated using quantitative comparison of four chemicals (deltamethrin, triphenyl phosphate, methyl mercuric (II) chloride, and saccharin) that were included in concentration-response on two separate plates. A comparison of the POD values for each chemical and all phenotypes is depicted in Figure 4B. Correlation analysis for inter-plate POD values revealed r values of 0.93 (for 11 phenotypes, including the 10 for

cardiophysiology and the one for cell viability after 24 hrs of exposure) and 0.91 (for the 7 cellular/mitochondrial toxicity phenotypes collected after 30 minutes of chemical exposure) and corresponding ρ values of 0.84 and 0.91. In all cases, the correlations were significant ($p<0.0001$).

A heatmap visualization of normalized peak frequency concentration-response data (Figure 5), a representative cardiophysiology phenotype, revealed that many of the 69 test chemicals had concentration-dependent effects on peak frequency while treatment of cardiomyocytes with the DMSO solvent control only or the negative controls biotin, sorbitol, and adipic acid did not alter this endpoint. For example, at 30 min, the pesticides dichlorodiphenyltrichloroethane (DDT), deltamethrin, dieldrin, and permethrin exhibited strong positive chronotropic effects at concentrations as low as 3 μM. Also at 30 min, other pesticides, including heptachlor, carbaryl, and carbamic acid, butyl-,3-iodo-2-propynl ester were capable of affecting peak frequency at 10 μM while captan, lindane, and parathion did so at 30 μM. Among the flame retardants tested at 30 min, nine of 10 induced positive chronotropic effects at concentrations between 3 and 30 μM; the exception was tris(2-chloroethyl) phosphate which was negative over the concentration range tested. The two most potent flame retardants, active at 3 μM, were 2-ethylhexyl diphenyl phosphate and tricresyl phosphate; the least potent, active at 30 μM, was 3,3′,5,5′-tetrabromobisphenol A. Of the 14 PAHs tested, 11 had a positive but generally weak effect on beat frequency at 10 and/or 30 μM; these included 4-H-cyclopenta(d,e,f)phenanthrene, acenaphthylene, benz(a)anthracene, benzo(a)pyrene, benzo(b)fluoranthene, benzo(e)pyrene, benzo(k)fluoranthene, fluorene, naphthalene, phenanthrene, and pyrene. Other chemicals, like 1-ethyl-3-methylimidazolium diethylphosphate, ‘acetic acid, manganese (2+) salt’, bisphenol A, di(2-ethylhexyl) phthalate, ‘manganese, tricarbonyl[(1,2,3,4,5-.eta.)-1-methyl-2,4-cyclopentadien-1-yl]-‘, methyl mercuric (II) chloride, n-hexane, saccharin sodium salt hydrate, and toluene, as well as the drugs 6-hydroxydopamine hydrochloride, 6-propyl-2-thiouracil, acetylsalicylic acid, berberine chloride, 1-methyl-4-phenypyridinium, diazepam, diethylstilbestrol, L-ascorbic acid, tetraethylthiuram disulfide, and valinomycin also altered peak frequency, albeit in many cases weakly. For each chemical, the normalized concentration response data and the corresponding numerical POD values for all endpoints are provided in Supplementary Tables 5 and 6, respectively.

At 30 min of exposure, several the tested chemicals (top cluster in Figure 5) exhibited non-monotonic concentration responses with initial increases in cardiomyocyte peak frequency followed by inhibition at a higher concentration; an effect that persisted for a subset of these chemicals for 24 hrs. Examples include the pesticides deltamethrin and the flame retardants isodecyl diphenyl phosphate and ‘phenol, isopropylated, phosphate (3:1)’. Importantly, at 30 min and at concentrations up to 30 μM, none of the tested chemicals had an effect on cell viability, whereas at 24 hrs, cytotoxicity was induced by 25 chemicals over the same concentration range. However, even at this time point, 32 chemicals (see Supplementary Table 6 for POD values <30 μM) exhibited an effect on peak frequency without decreasing cell viability.

It is important to note that seven chemicals, including the PAHs anthracene, benz(a)anthracene, benzo(e)pyrene, benzo(k)fluoranthene, and benzo(b)fluoranthene; the

solvent n-hexane; and the drug 3,3′-iminodipropionitrile exhibited a positive response in the Calcein AM readout (Figure 5), primarily at 24 hrs of exposure. While the effect was insignificant for 3,3′-iminodipropionitrile (calculated 24 hrs POD = 30 μM/nontoxic; Supplementary Table 6), it resulted in POD values below 30 μM for the other six chemicals. Considering the concordance of these findings among PAHs and across various other phenotypes (increases in nuclear intensity, no apparent change in nuclei numbers, see Supplementary Table 6), these effects might be biologically significant, albeit not directly interpretable as a cytotoxic response. As these findings affect subsequent analyses, we decided to adjust the POD values calculated for these chemicals for cardiotoxic selectivity assessment (which is based on cytotoxicity) to non-cytotoxic, i.e., 30 μM, but integrated the POD values into the assessment of biological similarity using ToxPi.

Cytotoxic effects of the test chemicals were evaluated using the cell viability dye Calcein AM and the Hoechst nuclear stain, the former at 24 hrs in cardiomyocytes evaluated for cardiophysiologic effects and both dyes at 30 min in cardiomyocytes evaluated for effects on mitochondria membrane potential. Other Hoechst nuclear stain read-outs at 30 min included total nuclei count, nuclear intensity, and total area of live cells. Early effects of chemicals on mitochondria membrane potential were evaluated using the mitochondria-specific marker JC-10; the mitochondria-specific descriptors were granules/cell, total granule area, and granular intensity. Mitochondrial depolarization is an early signal for hypoxic damage or oxidative stress (Dolman *et al.* 2013). Antimycin A, valinomycin, and CCCP, known disruptors of mitochondrial oxidative phosphorylation, were included as positive controls for this experiment. Representative images of control cells and cells treated with these chemicals, as well as those treated with methyl mercuric (II) chloride and deltamethrin are shown in Supplementary Figure 3.

Twenty-three chemicals disrupted mitochondria potential with POD values below 30 μM, as reflected by decreased numbers of granules per cell, average granule area, and/or granule intensity as compared to vehicle-treated controls (Supplementary Table 6), with decreases in granule intensity being the most common effect. These chemicals included the drugs berberine chloride, 3,3′-iminodipropionitrile, and valinomycin; the pesticides ‘carbamic acid, butyl-, 3-iodo-2-propynyl ester’, carbaryl, chlorpyrifos, dichlorodiphenyltrichloroethane (DDT), dieldrin, hexachlorphene, lindane, parathion, and tebuconazole; the flame retardants 2-ethylhexyl diphenyl phosphate, isodecyl diphenyl phosphate, ‘phenol, isopropylated, phosphate (3:1)’, tert-butylphenyl diphenyl phosphate, tricresyl phosphate, and triphenyl phosphate; the PAH fluorine; and the other chemicals methyl mercuric (II) chloride, 1-ethyl-3-methylimidazolium diethylphosphate, bisphenol A, and n-hexane. Interestingly, while the classical mitochondrial respiration uncoupler valinomycin exhibited a strong effect on mitochondria at 30 min after treatment, rotenone in this assay had no effect at this time point; however, both compounds were highly cytotoxic at 24 hrs. Rotenone did have pronounced effects, *i.e.* POD values of <30μM, in most other endpoints queried, including cytotoxicity, hence the lack of an observation for JC-10 at 30 min is an outlier in otherwise expected effects. Whether this lack of an effect is due to the sample time, cell type, or for other reasons requires further investigation.

A challenge and opportunity inherent to multidimensional screening data is related to the identification of chemicals that exert specific cardiotoxic effects as opposed to agents that exhibit tissue-nonspecific cytotoxicity. To determine if observed effects on intracellular Ca^{2+} flux were indeed specific indicators for physiological cardiomyocyte perturbation or were due to non-specific cytotoxicity or cell death (Judson *et al.* 2016; Thomas *et al.* 2013), we quantified the degree of specificity to parameter changes using a calculated selectivity score (Ryan *et al.* 2016). Cardiotoxic selectivity was calculated using the ratio between a POD for a cardiophysiologic phenotype and the associated decrease in cell viability, i.e., $POD_{cell\ viability}/POD_{Ca2+\ flux}$, across all five cardiophysiologic phenotypes and both time points. Chemicals were defined as "selective" if there was at least a three-fold difference (≥3) between a cardiophysiologic and a cytotoxic response, similar to a cutoff used by Judson *et al.* (2016). These values are provided in Supplementary Table 7 while the PODs for each endpoint are graphically presented in Figure 6, which ranks chemicals considered selective for cardiotoxicity by their selectivity score at 30 min and 24 hrs. At 30 min of exposure, 52 chemicals exhibited cardiotoxic selectivity for at least one of the five cardiophysiologic phenotypes, with the number of hits per phenotype being 43 for peak frequency and peak spacing, 42 for peak decay time, 41 for peak width, and 37 for peak rise time. Indeed, 31 of the 52 selective chemicals were selective across all five cardiophysiologic phenotypes, while 8, 1, 4, and 8 chemicals were selective for 4, 3, 2, and 1 cardiophysiologic phenotypes, respectively. Generally, for the chemicals that were selective for one cardiophysiologic phenotype only, the selectivity ratios were generally close to 3 with the exception being benzo(b)fluoranthracene with a selectivity ratio of ~2000 for an effect on peak rise time only. At 24 hrs of exposure, the overall number of compounds that exhibited selectivity for at least one of the cardiophysiologic phenotypes decreased to 45 with only 7 chemicals exhibiting a selective response across the 5 cardiophysiologic phenotypes. At this time point, the number of hits per phenotype were 20 for peak frequency, 21 for peak spacing, 27 for peak decay time, 17 for peak width, and 29 for peak rise time. The overall decreased concordance of cardiotoxic selectivity between the various phenotypes, resulting in only 7 chemicals being unanimous hits, is reflective of generally decreased selectivity ratios resulting from the presence of increased cytotoxicity and highlights the importance of including multiple cardiophysiologic phenotypes for the routine identification of selective cardiotoxic chemicals. These general trends are also observable for individual phenotypes, which were in many cases closely correlated (Supplementary Figure 4).

As a representative example, we show selectivity for chemical effects on cardiomyocyte beat frequency. Overall, 44 of the 69 unique chemicals had $POD_{Ca2+\ flux}$ values lower than 30 μM for peak frequency at 30 min of exposure (Supplementary Table 6). Of these, 43 exhibited selectivity for the effects on cardiomyocyte function versus cytotoxicity (Supplementary Table 6), i.e., the effects observed after short-term exposure were mostly due to the effects on calcium flux and not cytotoxicity. At 24 hrs of exposure, a greater number of chemicals (n=55) had $POD_{Ca2+\ flux}$ value lower than 30 μM, yet only 20 compounds remained selective with respect to the effects on Ca^{2+} flux as most were also cytotoxic. The 13 chemicals which were selective at both short-term (30 min) and longer-term exposures (24 hrs) were the drugs 1-methyl-4-phenylpyridinium iodide and berberine

chloride; the pesticides deltamethrin, permethrin, and rotenone; the flame retardants 2,2′, 4,4′-tetrabromodiphenyl ether, 2,2′,4,4′,5-pentabromodiphenyl ether, and 'phenol, isopropylated, phosphate (3:1)'; the PAHs acenaphthylene, fluorene, and pyrene; and two chemicals classified as other (di(2-ethylhexyl) phthalate and acetic acid, manganese (2+) salt. Thirty chemicals were selective at 30 min only, the most selective being valinomycin with a selectivity score of 8516.44, while 7 chemicals were selective at 24 hrs only, the most selective being benz(a)anthracene with a selectivity score of 86.01 (Supplementary Table 7). This temporal difference in the kinetics of chemical-induced cardiophysiologic effects at 30 min and 24 hrs supports the importance of the two time points when assessing the effect of chemicals on cardiophysiology *in vitro*.

To compare cardiotoxic potential of all chemicals tested in this study, we integrated and visualized POD data in ToxPi (Figure 7 and Supplementary Figure 5). POD values across multiple phenotypes served as quantitative measures of the relative bioactivity of chemicals within the current data set. ToxPi provides two types of outputs for each chemical included in the comparison. One is a relative bioactivity profile summarized in a pie chart where each slice is reflective of an individual phenotype while the slice area is proportional to the relative potency of the chemical as compared to the other chemicals in the data set. The second output is a ToxPi score representing the cumulative value for all slice areas of a given chemical. The ToxPi score is thus proportional to the relative bioactivity of a chemical within this dataset, a higher ToxPi score equals increased bioactivity; it was used for ranking the chemicals. A numerical list of all calculated ToxPi scores in this study can be found in Supplementary Table 8.

In a ToxPi analysis that included the 69 test chemicals along with assay-specific control chemicals, the positive and negative controls ranked at the top and bottom, respectively, as expected (Supplementary Figure 5A and Supplementary Table 8). The overall ranking of test chemicals according to their ToxPi score revealed some clustering of chemicals within the different chemical classes even though the ToxPi scores for the chemicals in each of the various chemical classes covered a broad range (drugs, 0.03 – 13.01, with valinomycin the most active; pesticides, 0.5 – 8.4 with rotenone being the most active; flame retardants, 0.7 – 5.2 with 2-ethylhexyl diphenyl phosphate being the most active; PAHs, 0.8 – 3.9 with benzo(a)pyrene being the most active; other chemicals, 0.3 – 6.9 with methyl mercuric (II) chloride being the most active (Figure 7) and their group mean ToxPi scores were not significantly different (Supplementary Figure 5B).

In contrast to the global ranking according to the cumulative ToxPi score, qualitative assessment of the individual toxicity profiles, i.e., ToxPi slices, revealed chemical class-specific characteristics (Figure 7). The pesticides parathion, tebuconazole, lindane, and chlorpyrifos formed a cluster of qualitatively similar bioactivity profiles, i.e. more profound, but moderate cardiophysiologic and mitochondrial effects after 30 min of exposure, as compared to the almost complete absence of cardiophysiologic effects and cytotoxicity after 24 hrs. Deltamethrin, permethrin, and rotenone are a second cluster of pesticides that may have effects on cardiophysiology with little to no cellular or mitochondrial toxicity. There also were some differences in the effects of the brominated and phosphate-containing flame retardant chemicals with the former exhibiting stronger potency in the functional assays of

cardiomyocytes; however, the small number of brominated agents tested precludes detailed comparative analysis. PAHs, including benzo(a)pyrene, benz(a)anthracene, benzo(k)fluoranthene, phenanthrene, and benzo(e)pyrene showed little to no cardiophysiologic effects after 30 min of exposure, but were associated with moderate cardiophysiologic effects after 24 hrs. This effect was not due to a decrease in cell viability, but several chemicals had a profound impact on the nuclear condensation concomitant to known pro-apoptosis effects (Puga *et al.* 2009).

In addition, we have POD values from all bioactivity phenotypes to reported human C_{max} values (for several drugs included in this screening) or *in vivo* blood concentration estimates derived from predictions of human exposure to environmental chemicals (Figure 8). Integration of dosimetry and exposure with high-throughput screening has been shown to aid in translating *in vitro* bioactivity concentrations to real-life exposures (Wetmore *et al.* 2015). Indeed, we observed that activity-to-exposure ratios for the environmental chemicals screened in this study ranged from one to five orders of magnitude, thus providing important information for a risk-based ranking strategy.

4. Discussion

Development and implementation of novel *in vitro* approaches for rapid hazard identification and dose-response analysis of environmental chemicals is an active area of toxicology (Judson *et al.* 2009; Judson *et al.* 2010; Tice *et al.* 2013). Human induced pluripotent stem cell-derived cell types, including iPSC-derived cardiomyocytes, have become an increasingly attractive as *in vitro* systems for both hazard evaluation and mechanistic toxicity studies due to their physiological relevance and unlimited supply as compared to primary cells or transformed cell lines (Acimovic *et al.* 2014; Anson *et al.* 2011; Mordwinkin *et al.* 2013; Sinnecker *et al.* 2014; Suter-Dick *et al.* 2015).

In this study, using two time points, a comprehensive *in vitro* cardiotoxicity evaluation was performed on a diverse library of 69 chemicals that included four major chemical classes with agents of known or suggested cardiotoxic potential: pesticides (Monge *et al.* 2005), flame retardants (Hassenklover *et al.* 2006; Lema *et al.* 2007), PAHs (Billiard *et al.* 2006; Burstyn *et al.* 2005), and drugs (Li *et al.* 2001). In addition to their cardiotoxic potential, these chemicals were selected to represent a diverse physico-chemical variety of environmentally available chemicals. Altogether, our cardiotoxicity evaluations of representative examples of these chemical classes indicate distinct, largely chemical class-specific effects on cardiophysiology, cytotoxicity, and mitochondrial depolarization. Our results are concordant with reports describing the potential for several of the drugs with the highest ToxPI scores [e.g., berberine chloride (Yan *et al.* 2015), valinomycin (Vogel and Sperelakis 1978), tetraethylthiuram disulfide (Fossa and Carlson, 1983), diethylstilbestrol (Martinez et al., 2001)] as well as environmental chemicals such as pesticides, flame retardants, PAHs, and others to possess cardiotoxic hazard (Billiard *et al.* 2006; Burstyn *et al.* 2005; Hassenklover *et al.* 2006; Lema *et al.* 2007; Monge *et al.* 2005).

While the cardiotoxic effects of many drugs are well-established, e.g. hERG channel inhibition resulting in prolonged repolarization/QT prolongation (Kamiya *et al.* 2006;

Sanguinetti and Tristani-Firouzi 2006) or β-adrenergic receptor stimulation resulting in positive inotropic effects (Chen-Izu *et al.* 2000), mechanisms are unknown or not clearly defined for most environmental chemicals but might include effects on ion channels (Narahashi 1996), the GABAA receptor chloride channel complex (Ogata *et al.* 1988), and voltage dependent Ca^{2+} currents (Hassenklover *et al.* 2006).

While a thorough mechanistic evaluation of the chemicals included in the screening library was not within the scope of the current study, the fact that chemical classes appeared to elicit overall qualitatively similar phenotypic toxicity profiles gives reason to speculate about common cardiotoxic pathways that are specifically targeted by distinct groups of environmental chemicals. For example, it would be reasonable to hypothesize that interference with ion channels may at least partially contribute to the positive and negative chronotropic effects (increase or decrease of the peak frequency) observed in the Ca^{2+} flux measurements. Drug-associated *in vivo* phenotypes, i.e. QT-elongation (cisapride), as well as positive (isoproterenol) and negative (propranolol) inotropic effects, can be reliably reproduced and quantified *in vitro* using the Ca^{2+} flux assay increases confidence in the biological relevance of the findings presented herein.

The inclusion of an imaging-based mitochondrial depolarization assay in this study represents an initial mechanistic attempt to evaluate the potential of chemicals to disrupt mitochondrial function. A variety of environmental chemicals, including the pesticides rotenone and chlorpyrifos, and the flame retardant tri-*ortho*-chresyl phosphate were previously identified as inhibitors of the mitochondrial electron transport chain, a pathway that can result in increased formation of reactive oxygen species and ultimately the induction of apoptosis (Jang *et al.* 2015; Zou *et al.* 2013). However, considering that cardiac mitochondrial effects of the majority of the chemicals included in the screening library have not been evaluated, it was important to characterize the effects of several other chemicals on mitochondria potential. Comparison of Ca^{2+} flux and mitochondria potential data (at 30 min of exposure) suggest that there might be a correlation between mitochondrial dysfunction and effects on the Ca^{2+} flux pattern. This is the case for a variety of chemicals, primarily flame retardants (e.g., 2-ethylhexyl diphenyl phosphate, ‘phenol, isopropylated phosphate (3:1)’, triphenyl phosphate) and certain pesticides (e.g., chlorpyrifos, lindane, parathion, tebuconazole), which selectively decreased mitochondria potential and showed effects on the cardiomyocyte beat pattern. While the direct link between mitochondria toxicity and the Ca^{2+} flux pattern is still to be established, there are reports indicating that mitochondria-related increases in cellular ROS may affect cardiomyocyte ion homeostasis, thereby contributing to the development of cardiac arrhythmias (Bovo *et al.* 2012; Liu *et al.* 2010).

A limitation of this assay, in common with most *in vitro* assays currently in use with the exception of those used for genotoxicity, is the lack of xenobiotic metabolism. Thus, the effects detected are due to the chemical tested and may not be relevant to *in vivo* situations. However, the developing ability to link organ-specific systems together make it likely that this limitation will be overcome in the very near future. One additional limitation is that iPSC-derived cardiomyocytes resemble fetal rather than adult cardiomyocytes (Gherghiceanu *et al.* 2011; Karakikes *et al.* 2015). Still, long-term culture of these cells (>2 months) leads to morphological maturation, i.e. a more rod-like shape as opposed to

spherical appearance, but the cardiomyocyte-associated beating still remains underdeveloped (Kamakura *et al.* 2013; Lundy *et al.* 2013). Also, differential cell culture conditions, as well as tissue engineering efforts have improved cellular metabolism to rely on beta oxidation as opposed to glycolysis, thereby mimicking the metabolism in adult ventricular cardiomyocytes (Drawnel *et al.* 2014; Wang *et al.* 2014). However, despite these apparent limitations, currently available iPSC-derived cardiomyocytes have clearly proven their utility and superiority over more conventional *in vitro* approaches in predicting chemical-induced cardiac functional and toxicity phenotypes and are widely accepted as a useful cardiotoxicity screening tool (Blinova *et al.* 2017; Guo *et al.* 2011; Karakikes *et al.* 2015; Mordwinkin *et al.* 2013).

In conclusion, our study is a comprehensive evaluation of a diverse set of environmental toxicants in a novel human organotypic cell culture model that not only has significant utility for cardiotoxicity screening, but is also widely used in drug safety evaluation (Anson *et al.* 2011; Lin and Will 2012). Cardiotoxicity testing is an unmet need in the current screening programs of environmental chemicals, but this study demonstrates that this iPSC-based cardiomyocyte platform is a robust, reproducible, and informative medium-throughput assay that can be incorporated into the Tox21 program (Tice *et al.* 2013). We show that the multiplexing of several orthogonal readouts – cardiomyocyte function, cell viability, nuclear morphology, and mitochondrial toxicity – at two exposure durations (30 min and 24 hrs) enables determination of the selectivity of the effects with respect to cardiomyocyte function, a path to address the challenge of interpretation of cell-based assays where the effects on a particular functional phenotype need to be dissociated from overall cell stress (Judson *et al.* 2016). Finally, the concentration-response profiling and derivation of quantitative POD estimates allows for ranking of compounds, and ultimate use of these data in risk-based evaluations by comparing the *in vitro* effects of chemicals and human exposure levels (Wambaugh *et al.* 2015).

Supplementary Material

Refer to Web version on PubMed Central for supplementary material.

Acknowledgments

The authors would like to acknowledge technical support and useful discussions with Carole Crittinden, Jayne Hesley, and Gabriele Mickevicius, as well as the useful comments of Drs. Michael DeVito and Erik Tokar at the NTP. The authors are grateful to Stephanie Holmgren at NIEHS for assistance with literature searches. This work was supported, in part, by a cooperative agreement STAR RD83580201 from US EPA to Texas A&M University. Drs. Behl, Parham, Ryan, and Tice were supported by the Intramural Research Program of the National Institutes of Health, National Institute of Environmental Health Sciences. The views expressed in this paper are those of the authors and do not necessarily reflect the views or policies of NIH. Mention of trade names or commercial products does not constitute endorsement or recommendation for use. Fabian Grimm was a recipient of the Society of Toxicology - Colgate-Palmolive Postdoctoral Fellowship Award in *In Vitro* Toxicology.

Abbreviations

CCCP	carbonyl cyanide m-chlorophenyl hydrazine
CDK	chemistry development kit

%CV	percent of the coefficient of variation
DDT	dichlorodiphenyltrichloroethane
DMSO	dimethyl sulfoxide
iPSC	induced pluripotent stem cell
POD	point-of-departure
PAH	polycyclic aromatic hydrocarbon
PCA	principal components analysis
ToxPi	toxicological priority index

References

Acimovic I, Vilotic A, Pesl M, Lacampagne A, Dvorak P, Rotrekl V, Meli AC. Human pluripotent stem cell-derived cardiomyocytes as research and therapeutic tools. Biomed Res Int. 2014; 2014:512831. [PubMed: 24800237]

Anson BD, Kolaja KL, Kamp TJ. Opportunities for use of human ips cells in predictive toxicology. Clin Pharmacol Ther. 2011; 89:754–758. [PubMed: 21430658]

Berridge BR, Hoffmann P, Turk JR, Sellke F, Gintant G, Hirkaler G, Dreher K, Schultze AE, Walker D, Edmunds N, Halpern W, Falls J, Sanders M, Pettit SD. Integrated and translational nonclinical in vivo cardiovascular risk assessment: Gaps and opportunities. Regul Toxicol Pharmacol. 2013; 65:38–46. [PubMed: 23044254]

Billiard SM, Timme-Laragy AR, Wassenberg DM, Cockman C, Di Giulio RT. The role of the aryl hydrocarbon receptor pathway in mediating synergistic developmental toxicity of polycyclic aromatic hydrocarbons to zebrafish. Toxicol Sci. 2006; 92:526–536. [PubMed: 16687390]

Blinova K, Stohlman J, Vicente J, Chan D, Johannesen L, Hortigon-Vinagre MP, Zamora V, Smith G, Crumb WJ, Pang L, Lyn-Cook B, Ross J, Brock M, Chvatal S, Millard D, Galeotti L, Stockbridge N, Strauss DG. Comprehensive translational assessment of human-induced pluripotent stem cell derived cardiomyocytes for evaluating drug-induced arrhythmias. Toxicol Sci. 2017; 155:234–247. [PubMed: 27701120]

Bovo E, Lipsius SL, Zima AV. Reactive oxygen species contribute to the development of arrhythmogenic ca(2) (+) waves during beta-adrenergic receptor stimulation in rabbit cardiomyocytes. J Physiol. 2012; 590:3291–3304. [PubMed: 22586224]

Burstyn I, Kromhout H, Partanen T, Svane O, Langard S, Ahrens W, Kauppinen T, Stucker I, Shaham J, Heederik D, Ferro G, Heikkila P, Hooiveld M, Johansen C, Randem BG, Boffetta P. Polycyclic aromatic hydrocarbons and fatal ischemic heart disease. Epidemiology. 2005; 16:744–750. [PubMed: 16222163]

Chen-Izu Y, Xiao RP, Izu LT, Cheng H, Kuschel M, Spurgeon H, Lakatta EG. G(i) -dependent localization of beta(2) -adrenergic receptor signaling to l-type ca(2+) channels. Biophys J. 2000; 79:2547–2556. [PubMed: 11053129]

Chen IY, Matsa E, Wu JC. Induced pluripotent stem cells: At the heart of cardiovascular precision medicine. Nat Rev Cardiol. 2016; 13:333–349. [PubMed: 27009425]

Collins FS, Gray GM, Bucher JR. Toxicology. Transforming environmental health protection. Science. 2008; 319:906–907. [PubMed: 18276874]

Dolman NJ, Chambers KM, Mandavilli B, Batchelor RH, Janes MS. Tools and techniques to measure mitophagy using fluorescence microscopy. Autophagy. 2013; 9:1653–1662. [PubMed: 24121704]

Drawnel FM, Boccardo S, Prummer M, Delobel F, Graff A, Weber M, Gerard R, Badi L, Kam-Thong T, Bu L, Jiang X, Hoflack JC, Kiialainen A, Jeworutzki E, Aoyama N, Carlson C, Burcin M, Gromo G, Boehringer M, Stahlberg H, Hall BJ, Magnone MC, Kolaja K, Chien KR, Bailly J,

Iacone R. Disease modeling and phenotypic drug screening for diabetic cardiomyopathy using human induced pluripotent stem cells. Cell Rep. 2014; 9:810–821. [PubMed: 25437537]

Gherghiceanu M, Barad L, Novak A, Reiter I, Itskovitz-Eldor J, Binah O, Popescu LM. Cardiomyocytes derived from human embryonic and induced pluripotent stem cells: Comparative ultrastructure. J Cell Mol Med. 2011; 15:2539–2551. [PubMed: 21883888]

Grimm FA, Iwata Y, Sirenko O, Bittner M, Rusyn I. High-content assay multiplexing for toxicity screening in induced pluripotent stem cell-derived cardiomyocytes and hepatocytes. Assay Drug Dev Technol. 2015; 13:529–546. [PubMed: 26539751]

Grimm FA, Iwata Y, Sirenko O, Chappell GA, Wright FA, Reif DM, Braisted J, Gerhold DL, Yeakley JM, Shepard P, Seligmann B, Roy T, Boogaard PJ, Ketelslegers H, Rohde A, Rusyn I. A chemical-biological similarity-based grouping of complex substances as a prototype approach for evaluating chemical alternatives. Green Chem. 2016; 18:4407–4419. [PubMed: 28035192]

Guo L, Abrams RM, Babiarz JE, Cohen JD, Kameoka S, Sanders MJ, Chiao E, Kolaja KL. Estimating the risk of drug-induced proarrhythmia using human induced pluripotent stem cell-derived cardiomyocytes. Toxicol Sci. 2011; 123:281–289. [PubMed: 21693436]

Guo L, Coyle L, Abrams RM, Kemper R, Chiao ET, Kolaja KL. Refining the human ipsc-cardiomyocyte arrhythmic risk assessment model. Toxicol Sci. 2013; 136:581–594. [PubMed: 24052561]

Hancox JC, McPate MJ, El Harchi A, Zhang YH. The herg potassium channel and herg screening for drug-induced torsades de pointes. Pharmacol Ther. 2008; 119:118–132. [PubMed: 18616963]

Hassenklover T, Predehl S, Pilli J, Ledwolorz J, Assmann M, Bickmeyer U. Bromophenols, both present in marine organisms and in industrial flame retardants, disturb cellular ca2+ signaling in neuroendocrine cells (pc12). Aquat Toxicol. 2006; 76:37–45. [PubMed: 16263183]

Herman EH, Ferrans VJ. Preclinical animal models of cardiac protection from anthracycline-induced cardiotoxicity. Semin Oncol. 1998; 25:15–21.

Hoekstra M, Mummery CL, Wilde AA, Bezzina CR, Verkerk AO. Induced pluripotent stem cell derived cardiomyocytes as models for cardiac arrhythmias. Front Physiol. 2012; 3:346. [PubMed: 23015789]

Jang Y, Lee AY, Jeong SH, Park KH, Paik MK, Cho NJ, Kim JE, Cho MH. Chlorpyrifos induces nlrp3 inflammasome and pyroptosis/apoptosis via mitochondrial oxidative stress in human keratinocyte hacat cells. Toxicology. 2015; 338:37–46. [PubMed: 26435000]

Jeyaraj D, Haldar SM, Wan X, McCauley MD, Ripperger JA, Hu K, Lu Y, Eapen BL, Sharma N, Ficker E, Cutler MJ, Gulick J, Sanbe A, Robbins J, Demolombe S, Kondratov RV, Shea SA, Albrecht U, Wehrens XH, Rosenbaum DS, Jain MK. Circadian rhythms govern cardiac repolarization and arrhythmogenesis. Nature. 2012; 483:96–99. [PubMed: 22367544]

Judson R, Richard A, Dix DJ, Houck K, Martin M, Kavlock R, Dellarco V, Henry T, Holderman T, Sayre P, Tan S, Carpenter T, Smith E. The toxicity data landscape for environmental chemicals. Environ Health Perspect. 2009; 117:685–695. [PubMed: 19479008]

Judson R, Houck K, Martin M, Richard AM, Knudsen TB, Shah I, Little S, Wambaugh J, Setzer RW, Kothiya P, Phuong J, Filer D, Smith D, Reif D, Rotroff D, Kleinstreuer N, Sipes N, Xia M, Huang R, Crofton K, Thomas RS. Analysis of the effects of cell stress and cytotoxicity on in vitro assay activity across a diverse chemical and assay space. Toxicol Sci. 2016; 153:409. [PubMed: 27605417]

Judson RS, Houck KA, Kavlock RJ, Knudsen TB, Martin MT, Mortensen HM, Reif DM, Rotroff DM, Shah I, Richard AM, Dix DJ. In vitro screening of environmental chemicals for targeted testing prioritization: The toxcast project. Environ Health Perspect. 2010; 118:485–492. [PubMed: 20368123]

Kamakura T, Makiyama T, Sasaki K, Yoshida Y, Wuriyanghai Y, Chen J, Hattori T, Ohno S, Kita T, Horie M, Yamanaka S, Kimura T. Ultrastructural maturation of human-induced pluripotent stem cell-derived cardiomyocytes in a long-term culture. Circ J. 2013; 77:1307–1314. [PubMed: 23400258]

Kamiya K, Niwa R, Mitcheson JS, Sanguinetti MC. Molecular determinants of herg channel block. Mol Pharmacol. 2006; 69:1709–1716. [PubMed: 16474003]

Karakikes I, Ameen M, Termglinchan V, Wu JC. Human induced pluripotent stem cell-derived cardiomyocytes: Insights into molecular, cellular, and functional phenotypes. Circ Res. 2015; 117:80–88. [PubMed: 26089365]

Kaufman JD, Morgan MS, Marks ML, Greene HL, Rosenstock L. A study of the cardiac effects of bromochlorodifluoromethane (halon 1211) exposure during exercise. Am J Ind Med. 1992; 21:223–233. [PubMed: 1536156]

Knollmann BC. Induced pluripotent stem cell-derived cardiomyocytes: Boutique science or valuable arrhythmia model? Circ Res. 2013; 112:969–976. discussion 976. [PubMed: 23569106]

Laverty H, Benson C, Cartwright E, Cross M, Garland C, Hammond T, Holloway C, McMahon N, Milligan J, Park B, Pirmohamed M, Pollard C, Radford J, Roome N, Sager P, Singh S, Suter T, Suter W, Trafford A, Volders P, Wallis R, Weaver R, York M, Valentin J. How can we improve our understanding of cardiovascular safety liabilities to develop safer medicines? Br J Pharmacol. 2011; 163:675–693. [PubMed: 21306581]

Lema SC, Schultz IR, Scholz NL, Incardona JP, Swanson P. Neural defects and cardiac arrhythmia in fish larvae following embryonic exposure to 2,2′,4,4′-tetrabromodiphenyl ether (pbde 47). Aquat Toxicol. 2007; 82:296–307. [PubMed: 17412433]

Li BX, Yang BF, Zhou J, Xu CQ, Li YR. Inhibitory effects of berberine on ik1, ik, and herg channels of cardiac myocytes. Acta Pharmacol Sin. 2001; 22:125–131. [PubMed: 11741516]

Li X, Nooh MM, Bahouth SW. Role of akap79/150 protein in beta1-adrenergic receptor trafficking and signaling in mammalian cells. J Biol Chem. 2013; 288:33797–33812. [PubMed: 24121510]

Lin Z, Will Y. Evaluation of drugs with specific organ toxicities in organ-specific cell lines. Toxicol Sci. 2012; 126:114–127. [PubMed: 22166485]

Liu M, Liu H, Dudley SC Jr. Reactive oxygen species originating from mitochondria regulate the cardiac sodium channel. Circ Res. 2010; 107:967–974. [PubMed: 20724705]

Lundy SD, Zhu WZ, Regnier M, Laflamme MA. Structural and functional maturation of cardiomyocytes derived from human pluripotent stem cells. Stem Cells Dev. 2013; 22:1991–2002. [PubMed: 23461462]

Ma J, Guo L, Fiene SJ, Anson BD, Thomson JA, Kamp TJ, Kolaja KL, Swanson BJ, January CT. High purity human-induced pluripotent stem cell-derived cardiomyocytes: Electrophysiological properties of action potentials and ionic currents. Am J Physiol Heart Circ Physiol. 2011; 301:H2006–2017. [PubMed: 21890694]

Mansouri K, Abdelaziz A, Rybacka A, Roncaglioni A, Tropsha A, Varnek A, Zakharov A, Worth A, Richard AM, Grulke CM, Trisciuzzi D, Fourches D, Horvath D, Benfenati E, Muratov E, Wedebye EB, Grisoni F, Mangiatordi GF, Incisivo GM, Hong H, Ng HW, Tetko IV, Balabin I, Kancherla J, Shen J, Burton J, Nicklaus M, Cassotti M, Nikolov NG, Nicolotti O, Andersson PL, Zang Q, Politi R, Beger RD, Todeschini R, Huang R, Farag S, Rosenberg SA, Slavov S, Hu X, Judson RS. Cerapp: Collaborative estrogen receptor activity prediction project. Environ Health Perspect. 2016; 124:1023–1033. [PubMed: 26908244]

Mercola M, Colas A, Willems E. Induced pluripotent stem cells in cardiovascular drug discovery. Circ Res. 2013; 112:534–548. [PubMed: 23371902]

Monge P, Partanen T, Wesseling C, Bravo V, Ruepert C, Burstyn I. Assessment of pesticide exposure in the agricultural population of costa rica. Ann Occup Hyg. 2005; 49:375–384. [PubMed: 15650018]

Mordwinkin NM, Burridge PW, Wu JC. A review of human pluripotent stem cell-derived cardiomyocytes for high-throughput drug discovery, cardiotoxicity screening, and publication standards. J Cardiovasc Transl Res. 2013; 6:22–30. [PubMed: 23229562]

Nadanaciva S, Will Y. Investigating mitochondrial dysfunction to increase drug safety in the pharmaceutical industry. Curr Drug Targets. 2011; 12:774–782. [PubMed: 21275886]

Narahashi T. Neuronal ion channels as the target sites of insecticides. Pharmacol Toxicol. 1996; 79:1–14. [PubMed: 8841090]

Ogata N, Vogel SM, Narahashi T. Lindane but not deltamethrin blocks a component of gaba-activated chloride channels. FASEB J. 1988; 2:2895–2900. [PubMed: 2458984]

Pearce RG, Setzer RW, Strope CL, Sipes NS, Wambaugh JF. Httk: R package for high-throughput toxicokinetics. Journal of Statistical Software. 2017 In press.

Pierson JB, Berridge BR, Brooks MB, Dreher K, Koerner J, Schultze AE, Sarazan RD, Valentin JP, Vargas HM, Pettit SD. A public-private consortium advances cardiac safety evaluation: Achievements of the hesi cardiac safety technical committee. J Pharmacol Toxicol Methods. 2013; 68:7–12. [PubMed: 23567075]

Pruss-Ustun, A., Corvalan, C. Preventing disease through healthy environments: Towards an estimate of the environmental burden of disease. Geneva, Switzerland: World Health Organization; 2006.

Puga A, Ma C, Marlowe JL. The aryl hydrocarbon receptor cross-talks with multiple signal transduction pathways. Biochem Pharmacol. 2009; 77:713–722. [PubMed: 18817753]

Reif DM, Sypa M, Lock EF, Wright FA, Wilson A, Cathey T, Judson RR, Rusyn I. Toxpi gui: An interactive visualization tool for transparent integration of data from diverse sources of evidence. Bioinformatics. 2013; 29:402–403. [PubMed: 23202747]

Roberts RA, Kavanagh SL, Mellor HR, Pollard CE, Robinson S, Platz SJ. Reducing attrition in drug development: Smart loading preclinical safety assessment. Drug Discov Today. 2014; 19:341–347. [PubMed: 24269835]

Ryan KR, Sirenko O, Parham F, Hsieh JH, Cromwell EF, Tice RR, Behl M. Neurite outgrowth in human induced pluripotent stem cell-derived neurons as a high-throughput screen for developmental neurotoxicity or neurotoxicity. Neurotoxicology. 2016; 53:271–281. [PubMed: 26854185]

Sanguinetti MC, Tristani-Firouzi M. Herg potassium channels and cardiac arrhythmia. Nature. 2006; 440:463–469. [PubMed: 16554806]

Sinnecker D, Laugwitz KL, Moretti A. Induced pluripotent stem cell-derived cardiomyocytes for drug development and toxicity testing. Pharmacol Ther. 2014; 143:246–252. [PubMed: 24657289]

Sirenko O, Crittenden C, Callamaras N, Hesley J, Chen YW, Funes C, Rusyn I, Anson B, Cromwell EF. Multiparameter in vitro assessment of compound effects on cardiomyocyte physiology using ipsc cells. J Biomol Screen. 2013a; 18:39–53. [PubMed: 22972846]

Sirenko O, Cromwell EF, Crittenden C, Wignall JA, Wright FA, Rusyn I. Assessment of beating parameters in human induced pluripotent stem cells enables quantitative in vitro screening for cardiotoxicity. Toxicol Appl Pharmacol. 2013b; 273:500–507. [PubMed: 24095675]

Steinbeck C, Han Y, Kuhn S, Horlacher O, Luttmann E, Willighagen E. The chemistry development kit (cdk) : An open-source java library for chemo- and bioinformatics. J Chem Inf Comput Sci. 2003; 43:493–500. [PubMed: 12653513]

Suter-Dick L, Alves PM, Blaauboer BJ, Bremm KD, Brito C, Coecke S, Flick B, Fowler P, Hescheler J, Ingelman-Sundberg M, Jennings P, Kelm JM, Manou I, Mistry P, Moretto A, Roth A, Stedman D, van de Water B, Beilmann M. Stem cell-derived systems in toxicology assessment. Stem Cells Dev. 2015; 24:1284–1296. [PubMed: 25675366]

Thomas RS, Philbert MA, Auerbach SS, Wetmore BA, Devito MJ, Cote I, Rowlands JC, Whelan MP, Hays SM, Andersen ME, Meek ME, Reiter LW, Lambert JC, Clewell HJ 3rd, Stephens ML, Zhao QJ, Wesselkamper SC, Flowers L, Carney EW, Pastoor TP, Petersen DD, Yauk CL, Nong A. Incorporating new technologies into toxicity testing and risk assessment: Moving from 21st century vision to a data-driven framework. Toxicol Sci. 2013; 136:4–18. [PubMed: 23958734]

Tice RR, Austin CP, Kavlock RJ, Bucher JR. Improving the human hazard characterization of chemicals: A tox21 update. Environ Health Perspect. 2013; 121:756–765. [PubMed: 23603828]

U.S. EPA. Benchmark dose technical guidance. Washington, DC: Risk Assessment Forum, US EPA; 2012.

Vogel S, Sperelakis N. Valinomycin blockade of myocardial slow channels is reversed by high glucose. Am J Physiol. 1978; 235:H46–51. [PubMed: 677328]

Wambaugh JF, Wetmore BA, Pearce R, Strope C, Goldsmith R, Sluka JP, Sedykh A, Tropsha A, Bosgra S, Shah I, Judson R, Thomas RS, Woodrow Setzer R. Toxicokinetic triage for environmental chemicals. Toxicol Sci. 2015; 147:55–67. [PubMed: 26085347]

Wang G, McCain ML, Yang L, He A, Pasqualini FS, Agarwal A, Yuan H, Jiang D, Zhang D, Zangi L, Geva J, Roberts AE, Ma Q, Ding J, Chen J, Wang DZ, Li K, Wang J, Wanders RJ, Kulik W, Vaz FM, Laflamme MA, Murry CE, Chien KR, Kelley RI, Church GM, Parker KK, Pu WT. Modeling the mitochondrial cardiomyopathy of barth syndrome with induced pluripotent stem cell and heart-on-chip technologies. Nat Med. 2014; 20:616–623. [PubMed: 24813252]

Wetmore BA, Wambaugh JF, Ferguson SS, Sochaski MA, Rotroff DM, Freeman K, Clewell HJ 3rd, Dix DJ, Andersen ME, Houck KA, Allen B, Judson RS, Singh R, Kavlock RJ, Richard AM, Thomas RS. Integration of dosimetry, exposure, and high-throughput screening data in chemical toxicity assessment. Toxicol Sci. 2012; 125:157–174. [PubMed: 21948869]

Wetmore BA, Wambaugh JF, Ferguson SS, Li L, Clewell HJ 3rd, Judson RS, Freeman K, Bao W, Sochaski MA, Chu TM, Black MB, Healy E, Allen B, Andersen ME, Wolfinger RD, Thomas RS. Relative impact of incorporating pharmacokinetics on predicting in vivo hazard and mode of action from high-throughput in vitro toxicity assays. Toxicol Sci. 2013; 132:327–346. [PubMed: 23358191]

Wetmore BA, Wambaugh JF, Allen B, Ferguson SS, Sochaski MA, Setzer RW, Houck KA, Strope CL, Cantwell K, Judson RS, LeCluyse E, Clewell HJ, Thomas RS, Andersen ME. Incorporating high-throughput exposure predictions with dosimetry-adjusted in vitro bioactivity to inform chemical toxicity testing. Toxicol Sci. 2015; 148:121–136. [PubMed: 26251325]

Yan M, Zhang K, Shi Y, Feng L, Lv L, Li B. Mechanism and pharmacological rescue of berberine-induced herg channel deficiency. Drug Des Devel Ther. 2015; 9:5737–5747.

Zafiropoulos A, Tsarouhas K, Tsitsimpikou C, Fragkiadaki P, Germanakis I, Tsardi M, Maravgakis G, Goutzourelas N, Vasilaki F, Kouretas D, Hayes A, Tsatsakis A. Cardiotoxicity in rabbits after a low-level exposure to diazinon, propoxur, and chlorpyrifos. Hum Exp Toxicol. 2014; 33:1241–1252. [PubMed: 24818614]

Zhang Y, Huang L, Zuo Z, Chen Y, Wang C. Phenanthrene exposure causes cardiac arrhythmia in embryonic zebrafish via perturbing calcium handling. Aquat Toxicol. 2013; 142–143:26–32.

Zou C, Kou R, Gao Y, Xie K, Song F. Activation of mitochondria-mediated apoptotic pathway in tri-ortho-cresyl phosphate-induced delayed neuropathy. Neurochem Int. 2013; 62:965–972. [PubMed: 23541999]

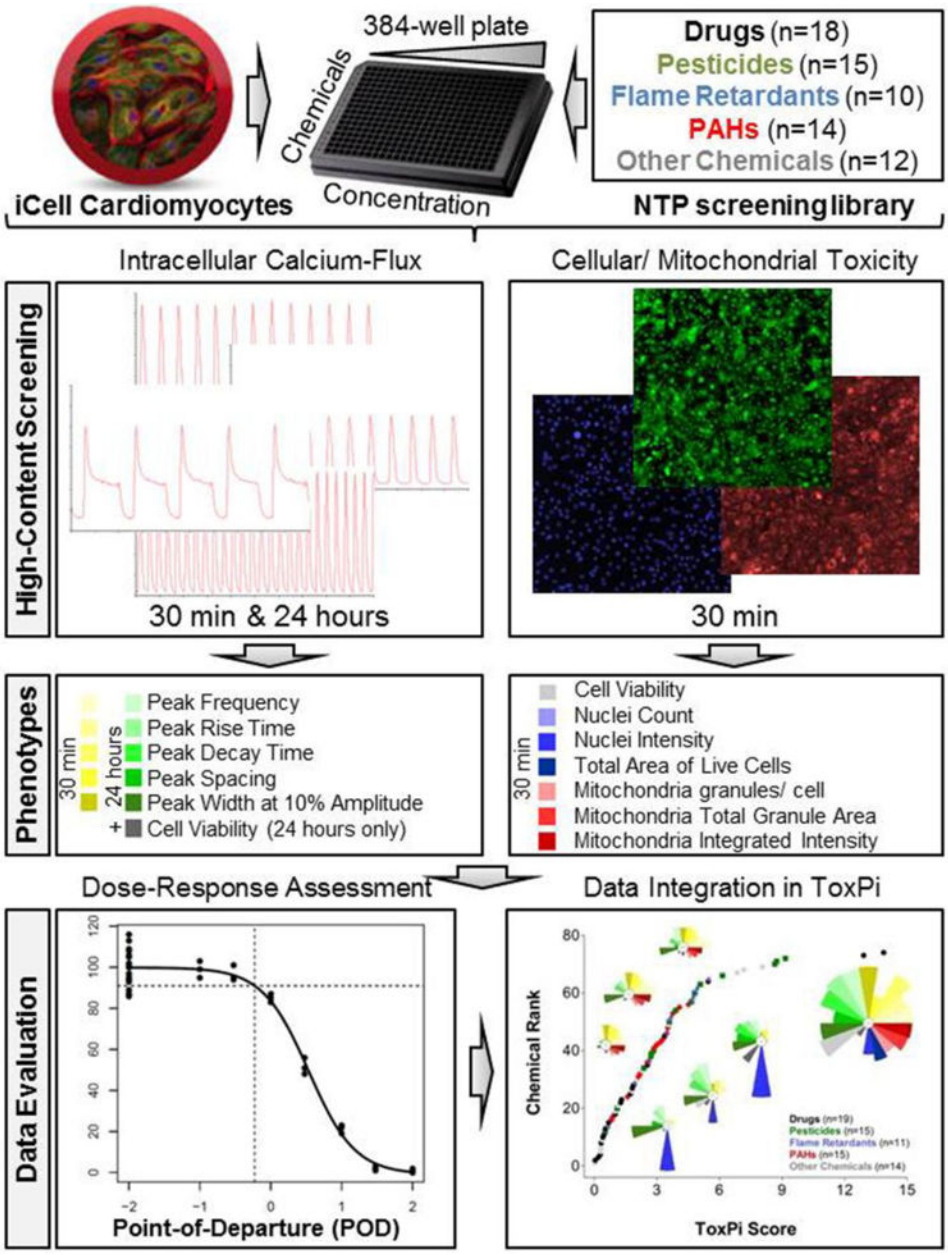

Figure 1.

Integrative *in vitro* assessment of cardiotoxicity. Induced pluripotent stem cell (iPSC)-derived cardiomyocytes were exposed to 86 environmental chemicals and drugs in concentration-response. Chemical effects on cardiomyocyte contractility were determined by intracellular calcium flux measurements after 30 min and 24 hrs of exposure. Using high-content fluorescence imaging, cellular toxicity was assessed after 30 min and 24 hrs while mitochondrial toxicity was assessed after 30 min. Phenotypic descriptors were used for quantitative concentration-response assessment and subsequent bioactivity profiling in ToxPi.

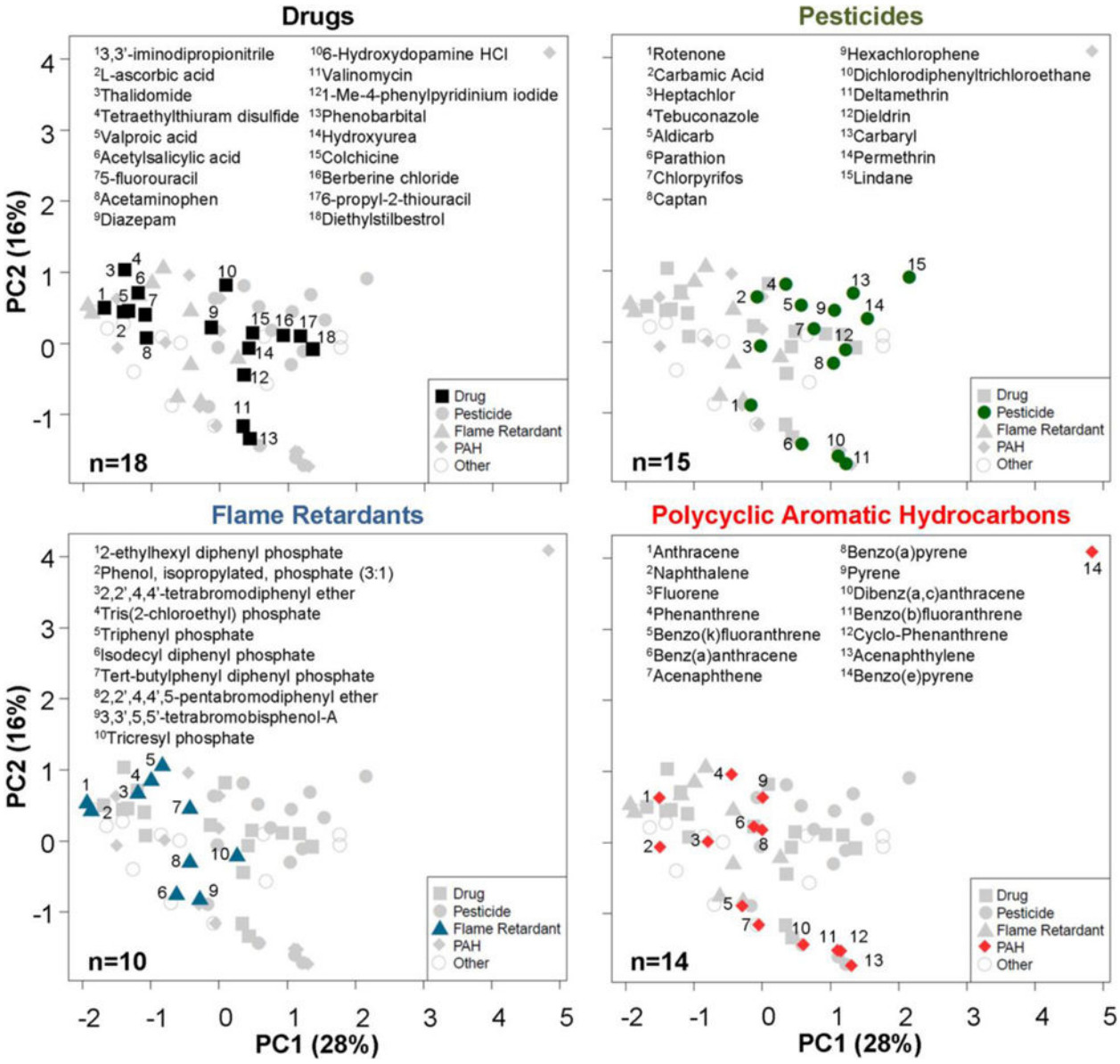

Figure 2.

Estimating the chemical diversity using physico-chemical descriptors. Principal components analysis of 153 physico-chemical descriptors calculated using Chembench web tool (https://chembench.mml.unc.edu/) reveals the chemical diversity of groups of chemicals used in this study. Mapping of the numbers in each panel to chemicals is provided in the inset above each graph.

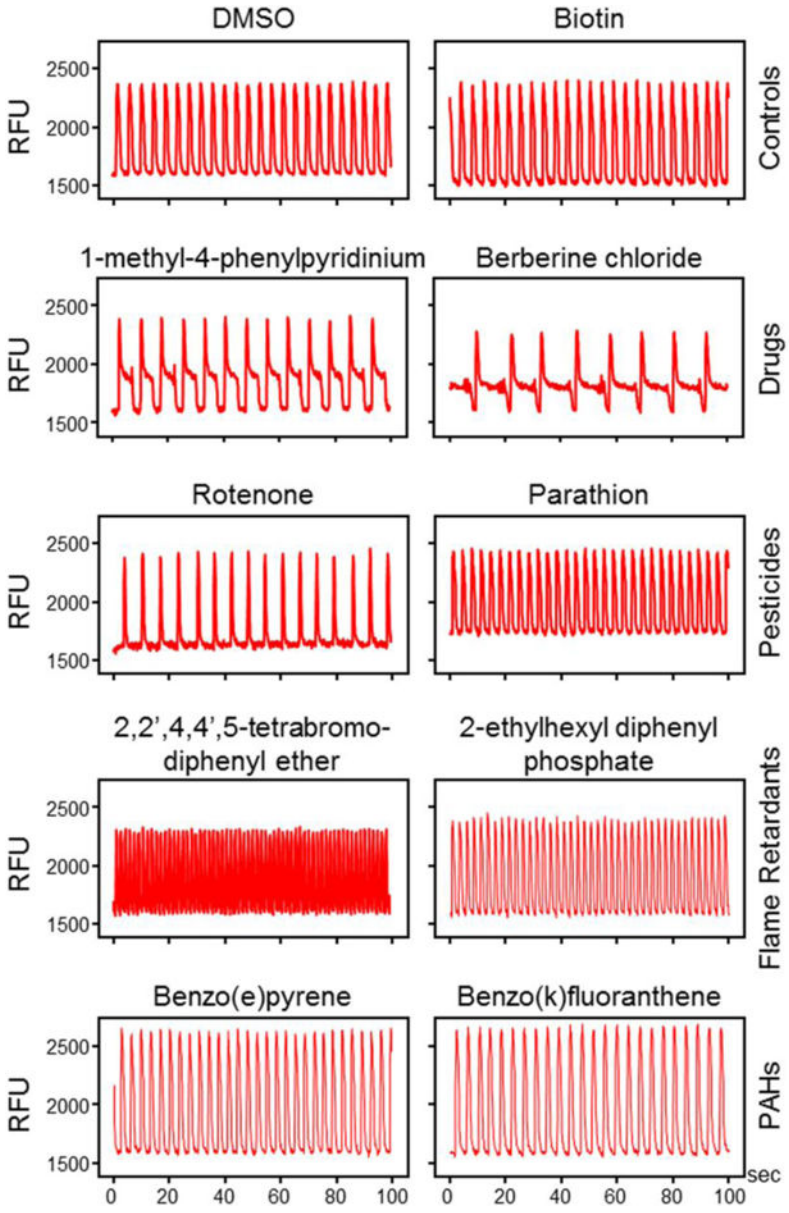

Figure 3.

Representative calcium-flux signal traces for different chemical classes. Shown are typical phenotypic responses including unaffected regular Ca2+-flux (DMSO, biotin) patterns, positive (the pesticide parathion, the flame retardants 2,2′,4,4′-tetrabromodiphenyl ether and 2-ethylhexyl diphenyl phosphate) and negative (the pesticide rotenone) inotropic effects, as well as prolongation of repolarization (the drugs 1-methyl-4-phenylpyridinium iodide and berberine chloride). The two polycyclic aromatic hydrocarbons (PAHs) benzo(e)pyrene and benzo(k)fluoranthene induce mild increases in peak frequency. Biotin, benzo(e)pyrene, benzo(k)fluoranthene traces presented for 30 μM concentrations, other chemicals for 10 μM concentrations after 30 minutes of exposure. [RFU=relative units of the fluorescence].

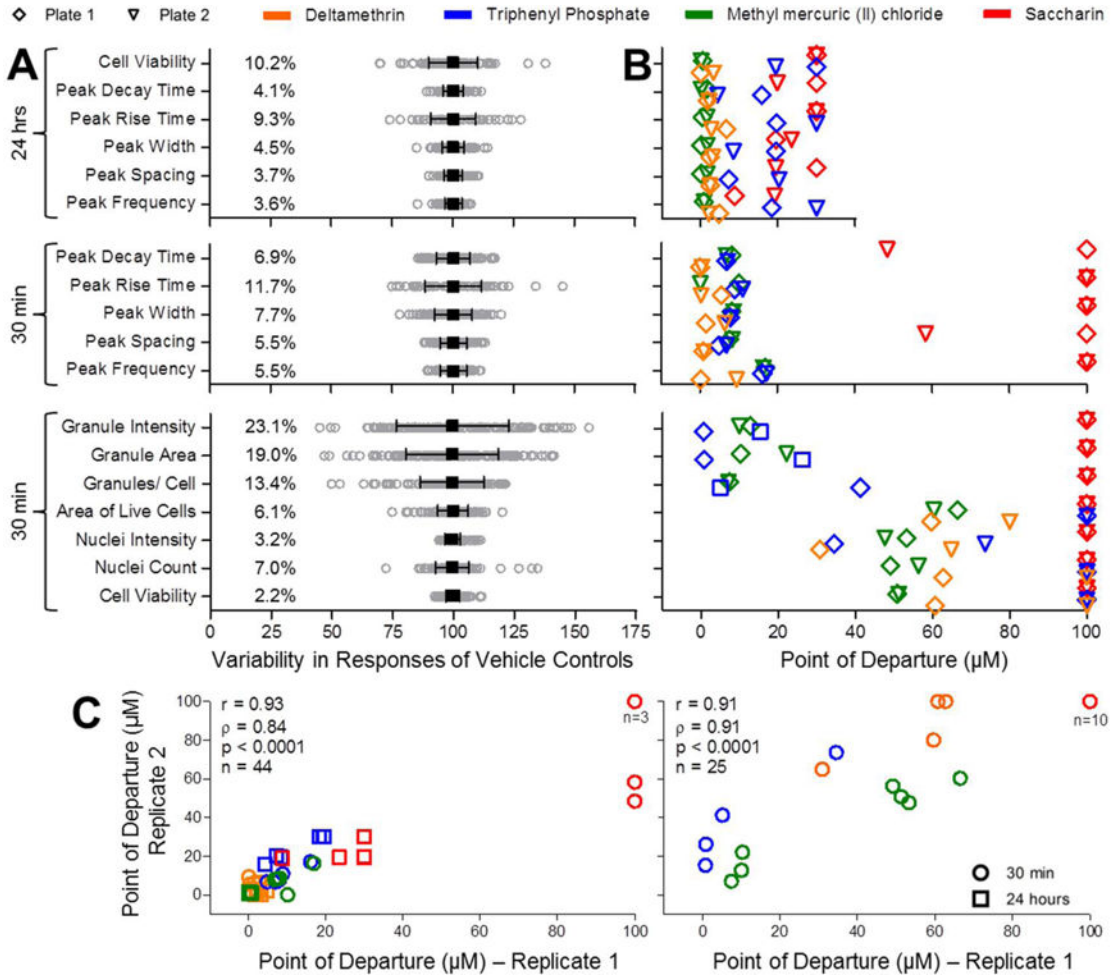

Figure 4.

Quality control of *in vitro* cardiotoxicity, cell viability, and mitochondrial toxicity assays. (A) Vehicle control (DMSO) variability (n=164 for Cardiophysiology at 30 min; n=116 for Cardiophysiology at 24 hrs; n=144 for Mitochondrial Toxicity). Mean (black square) ± SD (range bars) is shown for each phenotype overlaid on top of gray circles representing individual well responses. Coefficients of variation (%CV) are also shown for each phenotype. (B) Comparison of POD (Point-of-Departure) values from two different assay plates for deltamethrin, triphenyl phosphate, methyl mercuric (II) chloride, and saccharin. Plots indicate replicate PODs for 11 cardiophysiologic (n=44, including cell viability measurements after 24 hours) and 7 cellular and mitochondrial toxicities (n=25, all after 30 min of chemical exposure) phenotypes. Legend for plate and chemical identifiers is shown above the charts. (C) Correlation between inter-plate replicates for the above defined 11 cardiophysiologic (n=44, left) and 7 cellular and mitochondrial (n=25, right) was assessed using Pearson (r) and Spearman (ρ) analysis.

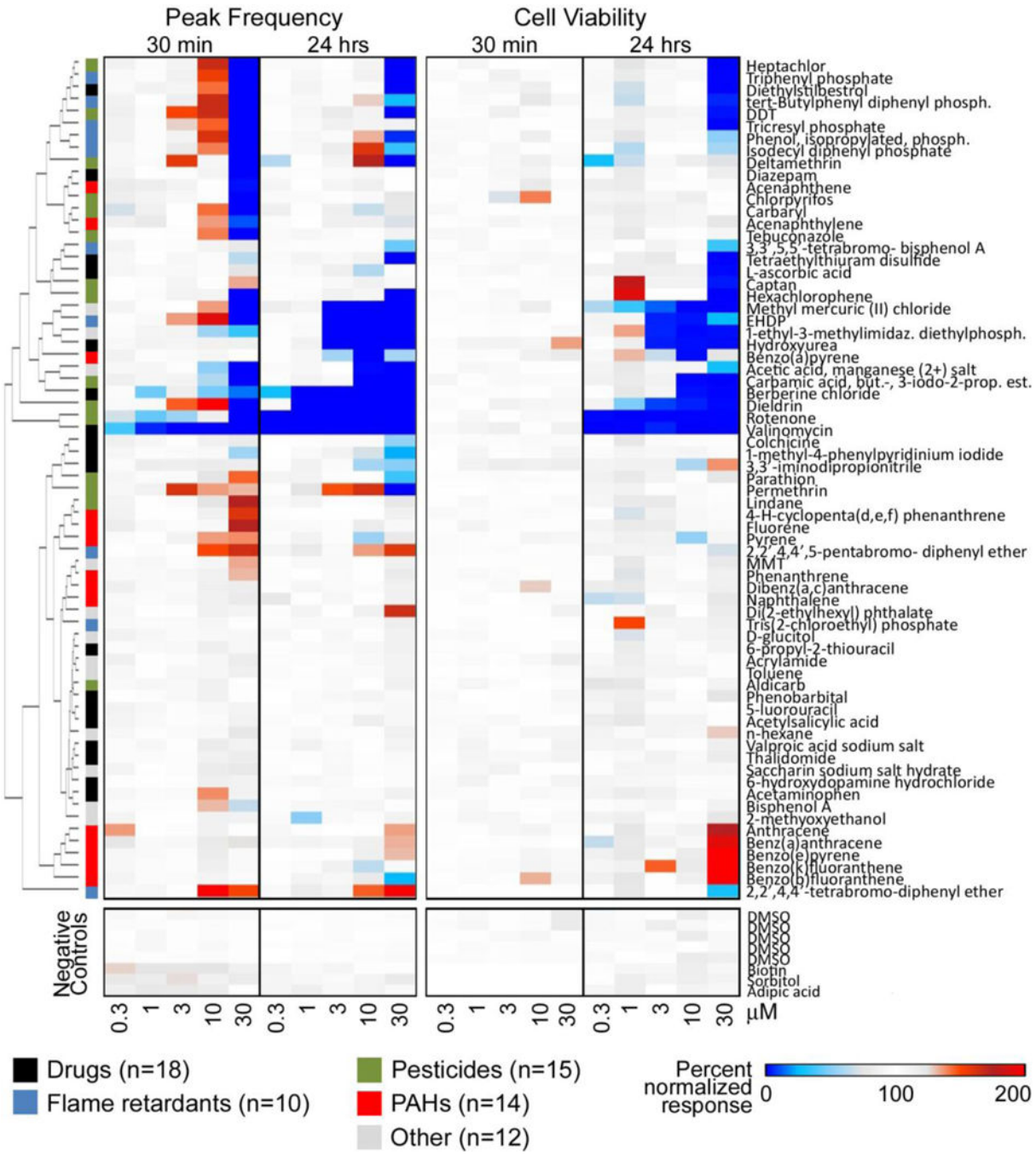

Figure 5.

Cluster analysis of quantitative concentration-response data for cardiomyocyte peak frequency and cell viability (0.3 – 30 µM data are shown). Responses at each time point and concentration are shown as a heat map (legend in the bottom of the figure). Chemical classes are also indicated by the colors next to the dendrogram. Full chemical names are indicated in Table 1 and Supplementary Table 1.

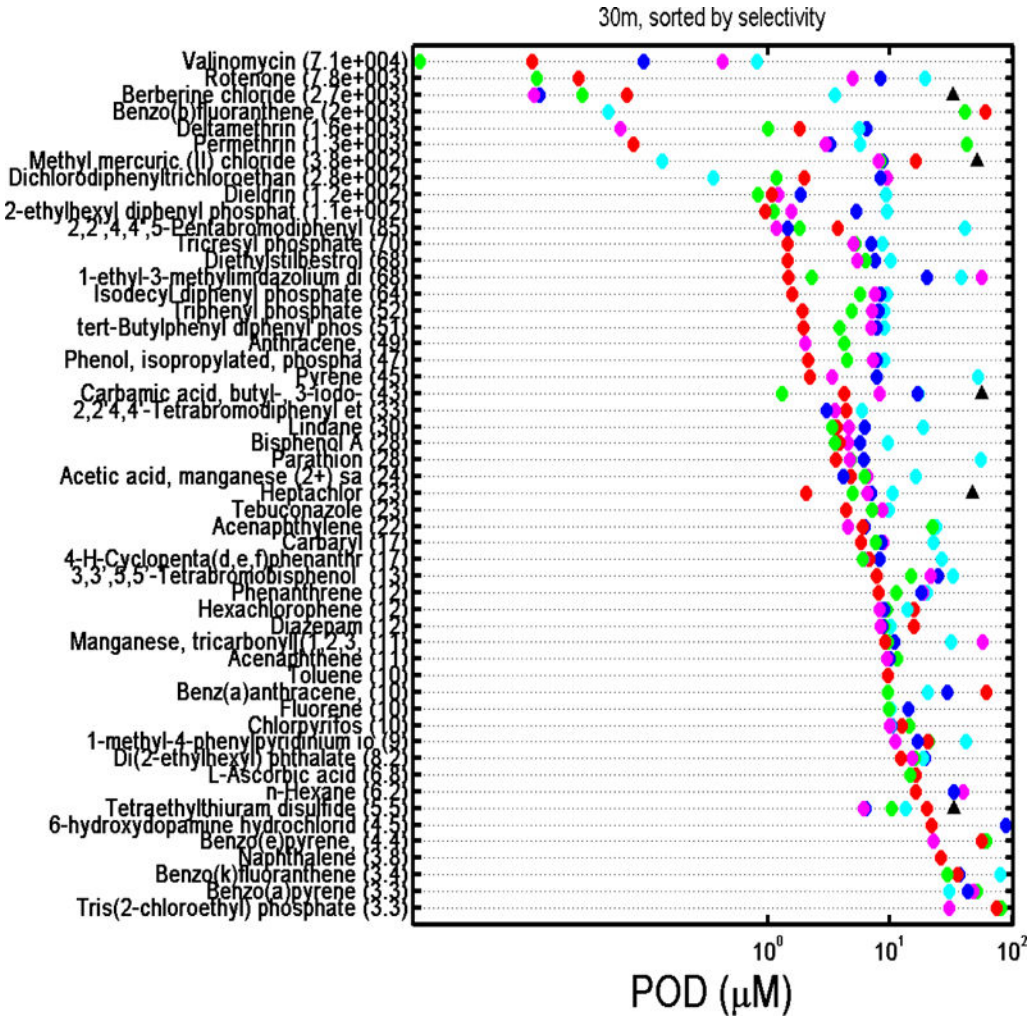

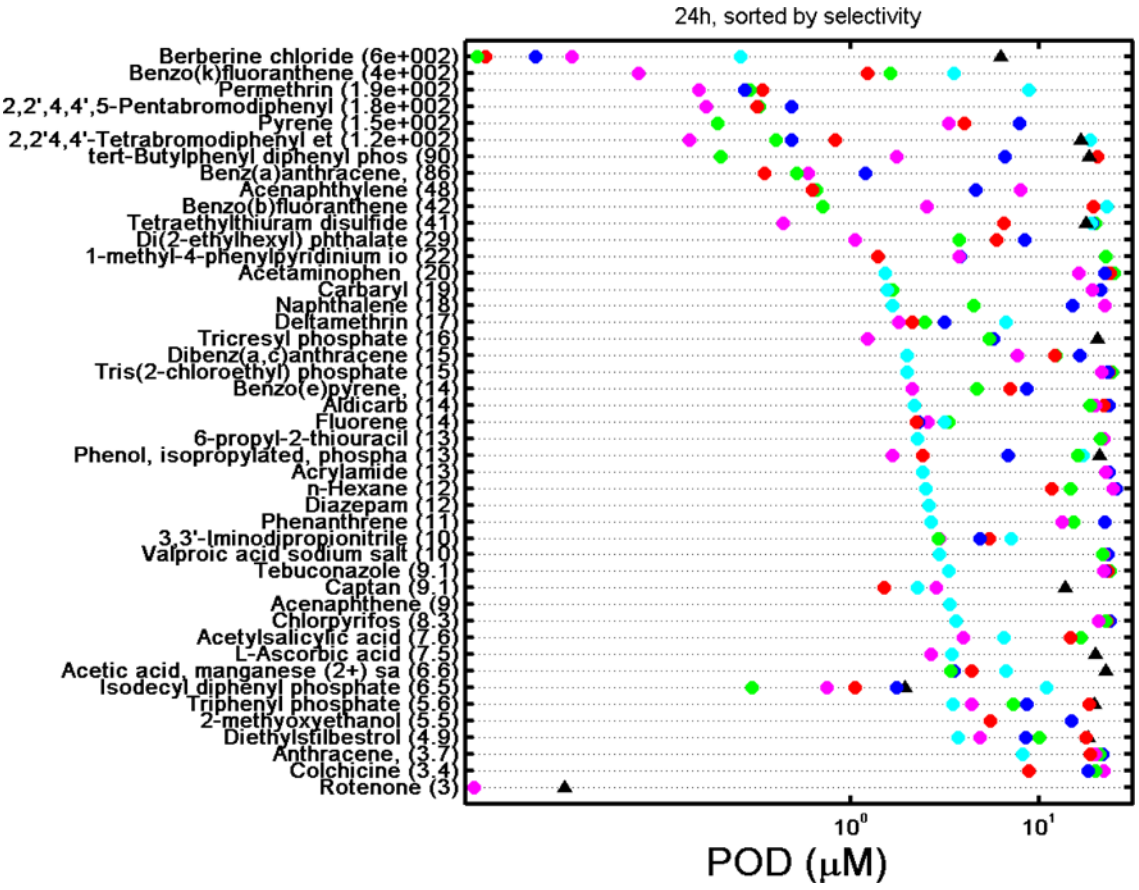

Figure 6.

A. Ranking of the 52 selective chemicals (i.e., chemicals with a $POD_{cell\ viability}$/$POD_{cardiophysiology}$ phenotype ratio ≥3) at 30 min by the greatest selectivity score (most selective compound on the top). Numbers in parenthesis is the selectivity ratio. Key: red circle = peak frequency; green circle = peak spacing; blue circle = peak width; cyan circle = peak rise time, magenta circle = peak decay time; black triangle = cell viability based on a decrease in Calcein AM signal. POD = point-of-departure concentrations.

B. Ranking of the 45 selective chemicals (i.e., chemicals with a $POD_{cell\ viability}$/$POD_{cardiophysiology}$ phenotype ratio ≥3) at 24 hrs by the greatest selectivity score (most selective compound on the top). Numbers in parenthesis is the selectivity ratio. Key: red circle = peak frequency; green circle = peak spacing; blue circle = peak width; cyan circle = peak rise time, magenta circle = peak decay time; black triangle = cell viability based on a decrease in Calcein AM signal. POD = point-of-departure concentrations.

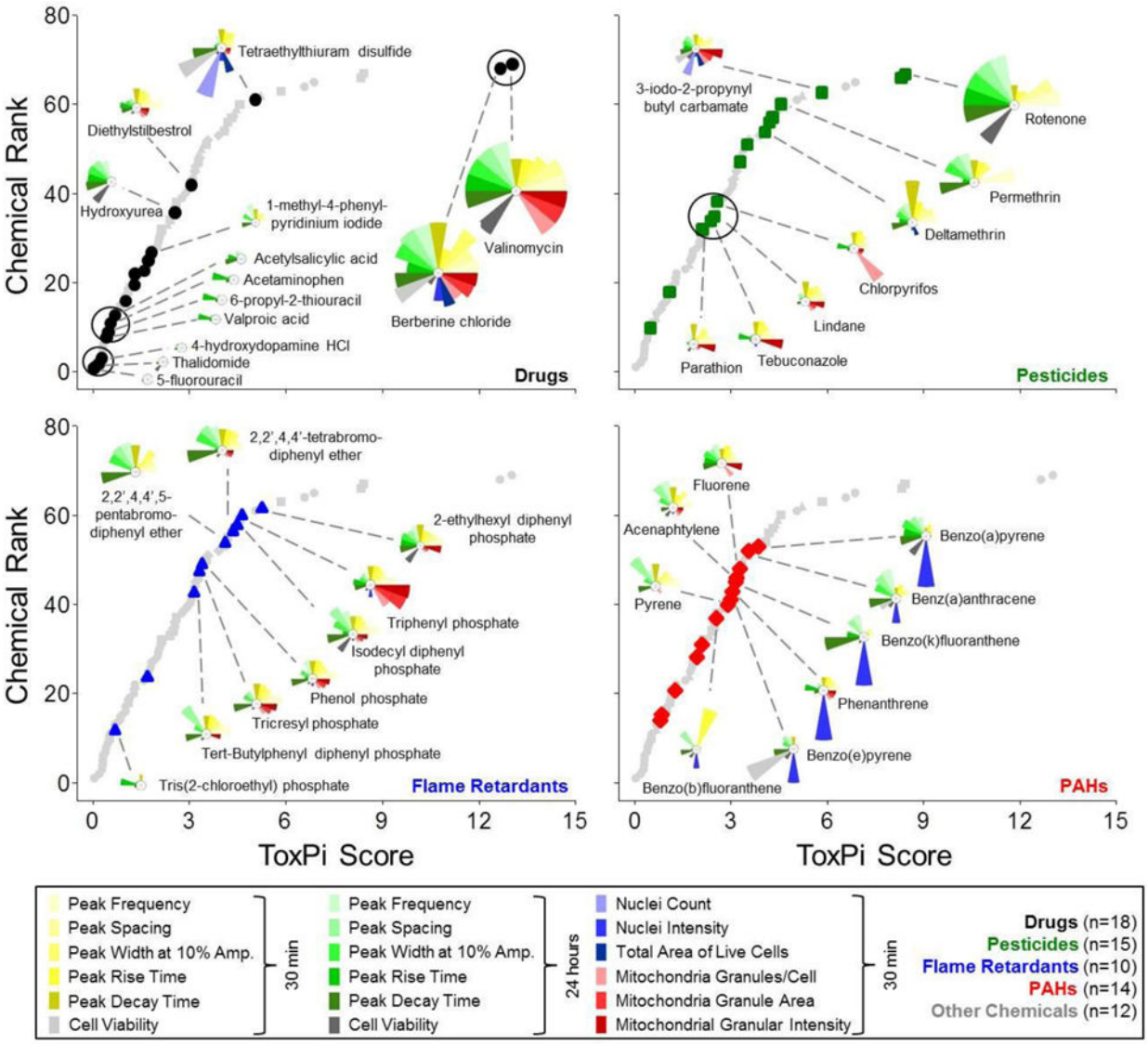

Figure 7.

Comprehensive ToxPi analysis of multiparametric cardiotoxicity assessment. POD (Point-of-Departure) values for 69 unique chemicals that were assessed for both cardiophysiology (10 phenotypes) and cellular/mitochondrial toxicity (8 phenotypes) were integrated in ToxPi software for quantitative bioactivity profiling. Plots indicate relative chemical rankings per chemical class. ToxPi profiles for selected representative chemicals are indicated.

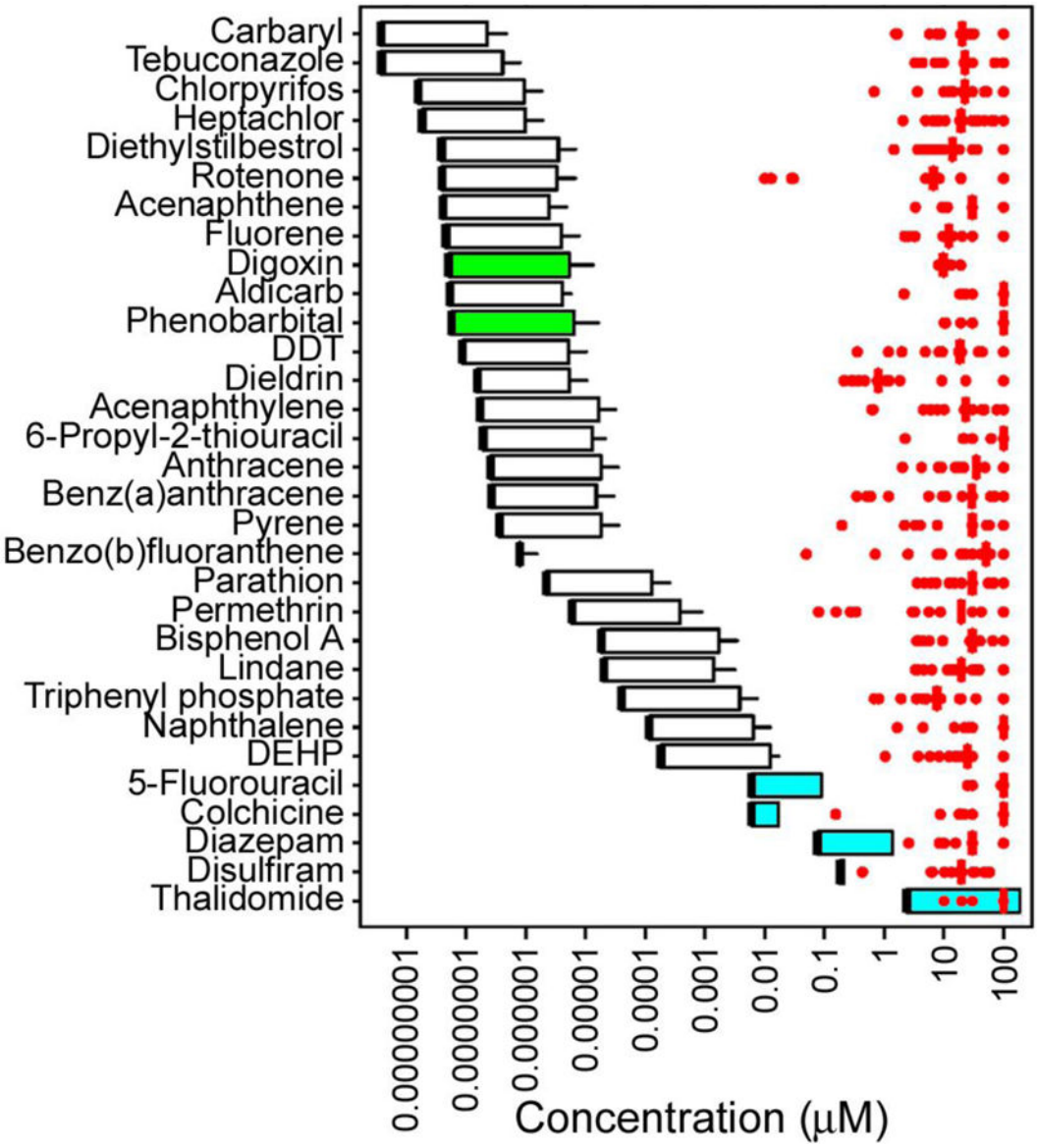

Figure 8.

Comparison of POD (Point-of-Departure) values for *in vitro* cardiotoxicity, cell viability, and mitochondrial toxicity assays (red dots are individual values, red vertical bar is the median) and human blood concentration estimates (box and whisker) for the chemicals analyzed. Blood concentration ranges for the chemicals shown were derived as detailed in Methods. Thick black line is the predicted blood concentration at median exposure assuming median toxicokinetics. Upper bound of the box is predicted blood concentration at the 95th percentile for exposure assuming median toxicokinetics. Whisker is predicted blood concentration at the 95th percentile for exposure assuming 95th percentile of toxicokinetics. White box and whisker graphs are for chemicals with the blood concentrations at steady state values as reported in Wetmore *et al.* (2015). Green box and whisker graphs are for chemicals with the blood concentrations at steady state values calculated using a 3

compartment model implemented by Pearce *et al.* (2017). Blue box and whisker graphs are for drugs with reported C_{max} ranges from human clinical trials.

Table 1

List of chemicals used for phenotypic screening.

Chemical Name	Category
1-Methyl-4-phenylpyridinium iodide (MPP+)	Drug
3,3′-Iminodipropionitrile	Drug
5-Fluorouracil	Drug
6-Hydroxydopamine hydrochloride	Drug
6-Propyl-2-thiouracil	Drug
Acetaminophen	Drug
Acetylsalicylic acid	Drug
Berberine chloride	Drug
Colchicine	Drug
Diazepam	Drug
Diethylstilbestrol	Drug
Hydroxyurea	Drug
L-Ascorbic acid	Drug
Phenobarbital	Drug
Tetraethylthiuram disulfide	Drug
Thalidomide	Drug
Valinomycin	Drug
Valproic acid sodium salt	Drug
Aldicarb	Pesticide
Captan	Pesticide
Carbamic acid, butyl-, 3-iodo-2-propynyl ester	Pesticide
Carbaryl	Pesticide
Chlorpyrifos	Pesticide
Deltamethrin	Pesticide
Dichlorodiphenyltrichloroethane (DDT)	Pesticide
Dieldrin	Pesticide
Heptachlor	Pesticide
Hexachlorophene	Pesticide
Lindane	Pesticide
Parathion	Pesticide
Permethrin	Pesticide
Rotenone	Pesticide
Tebuconazole	Pesticide
2- Ethylhexyl diphenyl phosphate (EHDP)	Flame Retardant
2,2′,4,4′,5-Pentabromodiphenyl ether	Flame Retardant
2,2′4,4′-Tetrabromodiphenyl ether	Flame Retardant
3,3′,5,5′-Tetrabromobisphenol A	Flame Retardant
Isodecyl diphenyl phosphate	Flame Retardant
Phenol, isopropylated, phosphate (3:1)	Flame Retardant

Chemical Name	Category
tert-Butylphenyl diphenyl phosphate	Flame Retardant
Tricresyl phosphate	Flame Retardant
Triphenyl phosphate	Flame Retardant
Tris(2-chloroethyl) phosphate	Flame Retardant
4-H-Cyclopenta(d,e,f)phenanthrene	PAH
Acenaphthene	PAH
Acenaphthylene	PAH
Anthracene	PAH
Benz(a)anthracene	PAH
Benzo(a)pyrene	PAH
Benzo(b)fluoranthene	PAH
Benzo(e)pyrene	PAH
Benzo(k)fluoranthene	PAH
Dibenz(a,c)anthracene	PAH
Fluorene	PAH
Naphthalene	PAH
Phenanthrene	PAH
Pyrene	PAH
Acrylamide	Other
Acetic acid, manganese (2+) salt	Other/Metal
Manganese, tricarbonyl[(1,2,3,4,5-.eta.)-1-methyl-2,4-cyclopentadien-1-yl]- (MMT)	Other/Metal
Methyl mercuric (II) chloride	Other/Metal
Bisphenol A	Other/Plasticizer
Di(2-ethylhexyl) phthalate	Other/Plasticizer
1-Ethyl-3-methylimidazolium diethylphosphate	Other/Plasticizer
2-Methyoxyethanol	Other/Solvent
n-Hexane	Other/Solvent
Toluene	Other/Solvent
D-Glucitol	Other/Sweetener
Saccharin sodium salt hydrate	Other/Sweetener
Biotin	Negative Control (Cardiophysiology)
Sorbitol	Negative Control (Cardiophysiology)
Adipic acid	Negative Control (Cardiophysiology)
Antimycin A	Positive Control (Mitochondrial Toxicant)
Digoxin	Positive Control (Mitochondrial Toxicant)
Carbonyl cyanide m-chlorophenyl hydrazone (CCCP)	Positive Control (Mitochondrial Toxicant)

Abbreviations: PAH = polycyclic aromatic hydrocarbon.